

State of the Global Climate 2024



WEATHER CLIMATE WATER



WORLD
METEOROLOGICAL
ORGANIZATION

WMO-No. 1368

WMO-No. 1368

© World Meteorological Organization, 2025

The right of publication in print, electronic and any other form and in any language is reserved by WMO. Short extracts from WMO publications may be reproduced without authorization, provided that the complete source is clearly indicated. Editorial correspondence and requests to publish, reproduce or translate this publication in part or in whole should be addressed to:

Chair, Publications Board
World Meteorological Organization (WMO)
7 bis, avenue de la Paix
P.O. Box 2300
CH-1211 Geneva 2, Switzerland

Tel.: +41 (0) 22 730 84 03
Email: publications@wmo.int

ISBN 978-92-63-11368-9

Cover illustration from Adobe Stock by Richie Chan: Scenery of Ghandruk village near Pokhara in Nepal

The designations employed and the presentation of material herein do not imply the expression of any opinion whatsoever on the part of the Secretariats of WMO or the United Nations concerning the legal status of any country, area or territory, or of its authorities, or concerning the delimitation of its borders. The depiction and use of boundaries, geographic names and related data on maps and in lists, tables, documents and databases herein are not warranted to be error-free and do not imply official endorsement or acceptance by WMO or the United Nations.

The mention of specific companies or products does not imply that they are endorsed or recommended by WMO in preference to others of a similar nature which are not mentioned or advertised.

The findings, interpretations and conclusions expressed in WMO publications with named authors are those of the authors alone and do not necessarily reflect those of WMO or its Members.

Contents

Foreword	ii
Key indicators.	1
Atmospheric carbon dioxide	1
Global mean near-surface temperature	3
Ocean heat content	5
Global mean sea level.	7
Ocean pH.	9
Glacier mass balance	11
Sea-ice extent	13
Climate driver – El Niño–Southern Oscillation	15
Global patterns of temperature and precipitation	17
Temperature	17
Precipitation	18
High-impact events	19
Monitoring global temperature for the Paris Agreement.	21
Global mean surface temperature anomalies in 2023/2024:	
Towards understanding the influencing factors.	23
Datasets and methods.	25
List of contributors.	31
Endnotes	34

We need your feedback

This year, the WMO team has launched a process to gather feedback on the *State of the Climate* reports and areas for improvement. Once you have finished reading the publication, we ask that you kindly give us your feedback by responding to [this short survey](#). Your input is highly appreciated.

Foreword



The annually averaged global mean near-surface temperature in 2024 was $1.55\text{ }^{\circ}\text{C} \pm 0.13\text{ }^{\circ}\text{C}$ above the 1850–1900 average. This is the warmest year in the 175-year observational record, beating the previous record set only the year before. While a single year above $1.5\text{ }^{\circ}\text{C}$ of warming does not indicate that the long-term temperature goals of the Paris Agreement are out of reach, it is a wake-up call that we are increasing the risks to our lives, economies and the planet.

Over the course of 2024, our oceans continued to warm, sea levels continued to rise, and acidification increased. The frozen parts of Earth's surface, known as the cryosphere, are melting at an alarming rate: glaciers continue to retreat, and Antarctic sea ice reached the second-lowest extent ever recorded. Meanwhile, extreme weather continues to have devastating consequences around the world.

In response, WMO and the global community are intensifying efforts to strengthen early warning systems and climate services to help decision-makers and society at large be more resilient to extreme weather and climate. We are making progress but need to go further and need to go faster. Only half of all countries worldwide have adequate multi-hazard early warning systems. This must change.

Investment in National Meteorological and Hydrological Services is more important than ever to meet the challenges and build safer, more resilient communities. Authoritative scientific information and knowledge is necessary to inform decision-making in our rapidly changing world, and this report provides the latest science-based update on the state of our knowledge of key climate indicators.

A handwritten signature in black ink, likely belonging to Prof. Celeste Saulo.

(Prof. Celeste Saulo)
Secretary-General

Key indicator

Atmospheric carbon dioxide

KEY MESSAGES

- In 2023, the atmospheric concentration of carbon dioxide, as well as those of methane and nitrous oxide, reached the highest levels in the last 800 000 years.
- Real-time data from specific locations show that levels of these three main greenhouse gases continued to increase in 2024.

STATE OF THE INDICATOR

The global annual average mole fraction of carbon dioxide (CO₂) in the atmosphere – the atmospheric concentration – reached a new observed high in 2023, the latest year for which consolidated global annual figures are available (Figure 1). At 420.0 ± 0.1 parts per million (ppm), the concentration in 2023 was 2.3 ppm more than in 2022 and 151% of the pre-industrial concentration (in 1750).¹ The concentration of 420 ppm corresponds to 3 276 Gt CO₂ in the atmosphere.

Between 1 January 2023 and 31 December 2023, the concentration of CO₂ increased by 2.8 ppm, the fourth largest within-year change since modern CO₂ measurements started in the 1950s. The rate of growth is typically higher during El Niño conditions due to an overall increase from fire emissions and reduced net terrestrial carbon sinks (see [Climate Driver – El Niño–Southern Oscillation](#)).

Concentrations of methane (CH₄) and nitrous oxide (N₂O), two other key greenhouse gases, also reached record high observed levels in 2023. The concentration of CH₄ reached $1\,934 \pm 2$ parts

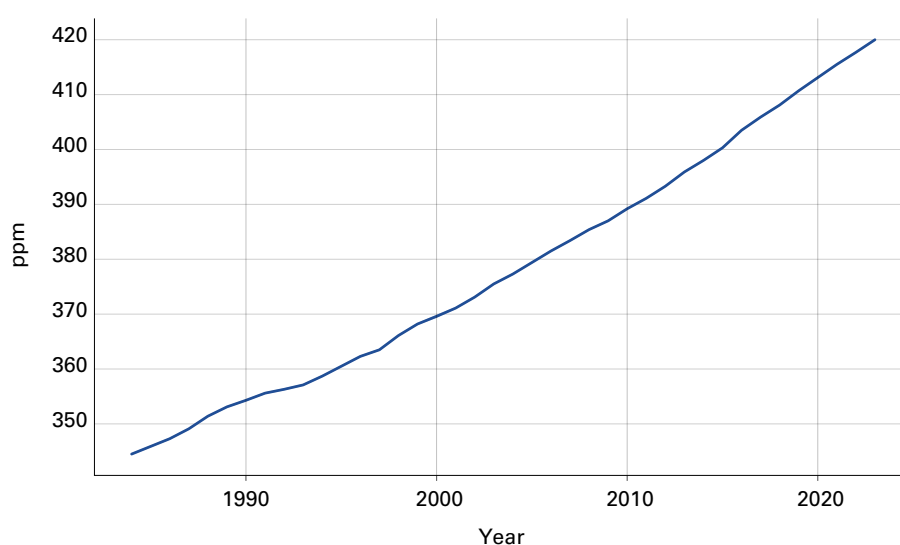


Figure 1. Annual mean globally averaged atmospheric mole fraction of carbon dioxide from 1984 to 2023 in parts per million (ppm)

Source: Data are from the World Data Centre for Greenhouse Gases (WDCGG). See [Datasets and methods](#).

per billion (ppb), 265% of pre-industrial levels, and that of N₂O reached 336.9 ± 0.1 ppb, 125% of pre-industrial levels. Real-time data show that levels of CO₂, CH₄ and N₂O continued to increase in 2024.

INDICATOR BACKGROUND

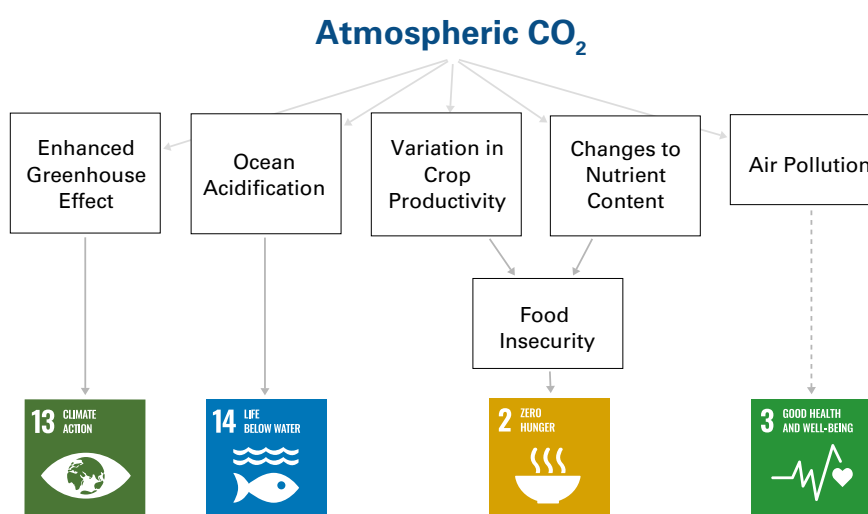
The human-caused increase in the concentration of CO₂ in the atmosphere is the largest driver of climate change. CO₂ accounts for around 66% of the radiative forcing by all long-lived greenhouse gases since 1750 and about 79% of the increase over the past decade.² Current atmospheric concentrations of CO₂ are higher than at any time in at least 2 million years.³ Concentrations of CH₄ and N₂O are higher than at any time in at least 800 000 years.

The concentrations of greenhouse gases presented here (Figure 1) are estimated from measurements made across a globally coordinated network covering the period 1984–2023. Pre-industrial concentrations (in 1750) are estimated using air trapped in ice cores.

Atmospheric concentrations of CO₂ reflect a balance between CO₂ sources and sinks. The anthropogenic sources of CO₂ are related to the burning of fossil fuel and cement production along with land use changes such as deforestation. Sinks of CO₂ include uptake by vegetation and the ocean.

The portion of CO₂ emitted by human activities that remains in the atmosphere is known as the airborne fraction. It varies from year to year due to the high natural variability of CO₂ sinks, in particular those on land. Natural sources and sinks of CO₂ are also affected by climate change via increasing temperature, and changes in precipitation and susceptibility to biomass burning.

During the 2014–2023 period, 48% of the total emissions from human activities remained in the atmosphere, driving the increase in atmospheric concentration. The estimated ocean sink accounted for 26% of emissions and the estimated land sink accounted for 30%.⁴



Associated risks of atmospheric CO₂ and the Sustainable Development Goals

Key indicator

Global mean near-surface temperature

KEY MESSAGES

- The annually averaged global mean near-surface temperature in 2024 was $1.55^{\circ}\text{C} \pm 0.13^{\circ}\text{C}$ above the 1850–1900 average used to represent pre-industrial conditions.
- The year 2024 was the warmest year in the 175-year observational record, clearly surpassing the previous warmest year, 2023 at $1.45^{\circ}\text{C} \pm 0.12^{\circ}\text{C}$ above the 1850–1900 average.
- For global mean temperature, each of the past ten years, 2015–2024, were individually the ten warmest years on record.

STATE OF THE INDICATOR

The annually averaged global mean near-surface temperature in 2024 was $1.55^{\circ}\text{C} \pm 0.13^{\circ}\text{C}$ above the 1850–1900 average. The year 2024 was the warmest year in the 175-year observational record. The previous warmest year was 2023 with an anomaly of $1.45^{\circ}\text{C} \pm 0.12^{\circ}\text{C}$. Each of the past ten years, 2015–2024, were individually the ten warmest years on record. The analysis is based on a synthesis of six global temperature datasets (Figure 2).

A single year with an annual global mean temperature over 1.5°C above the 1850–1900 average does not indicate that we have exceeded the warming levels from the Paris Agreement (see [Monitoring global temperature for the Paris Agreement](#)).

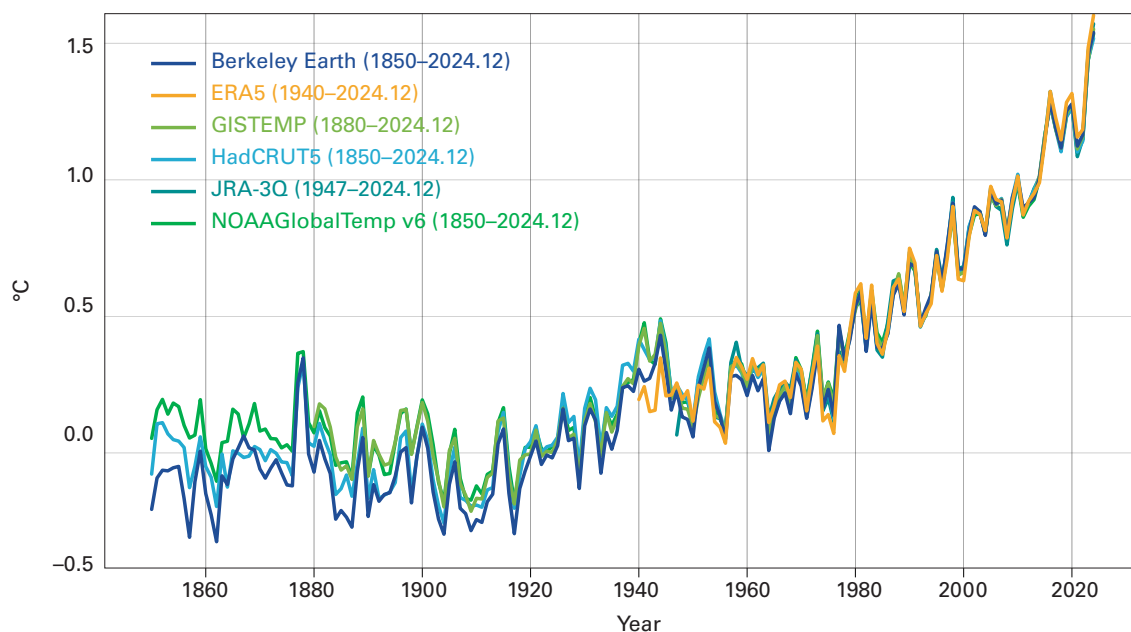


Figure 2. Annual global mean temperature anomalies relative to a pre-industrial (1850–1900) baseline shown from 1850 to 2024

Source: Data are from the six datasets indicated in the legend. For details see [Datasets and methods](#).

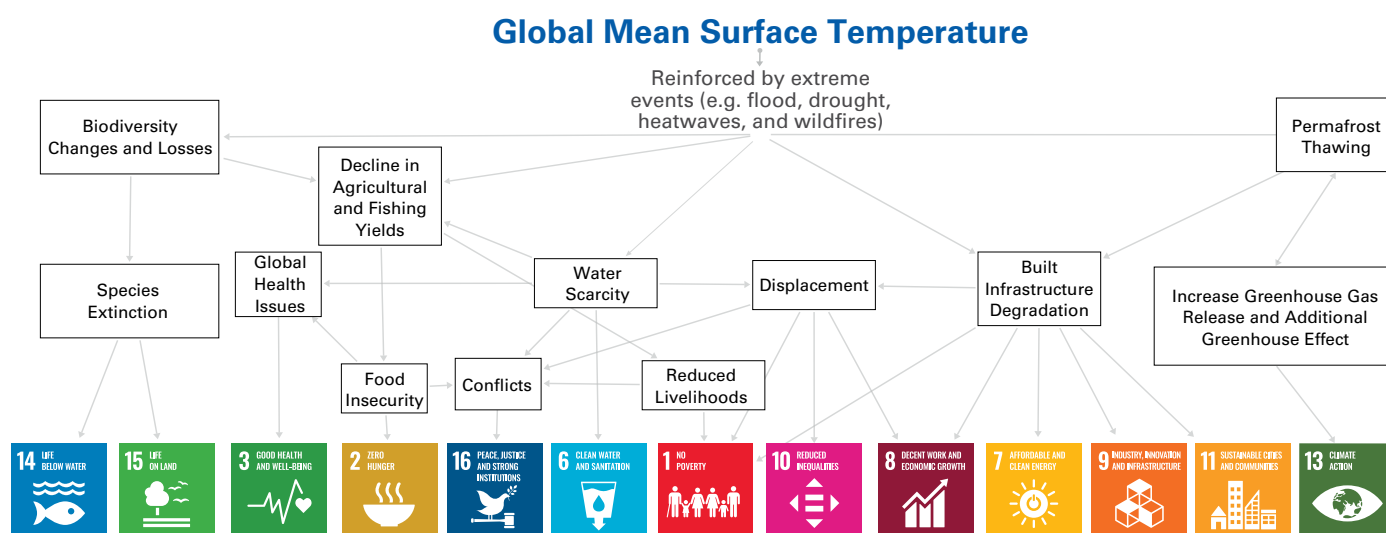
Global mean temperature in 2024 was boosted by a strong El Niño which peaked at the start of the year. However, temperatures were already at record levels in 2023 (see sidebar on [Global mean surface temperature anomalies in 2023/2024](#)). In every month between June 2023 and December 2024, monthly average global temperatures exceeded all monthly records prior to 2023.

INDICATOR BACKGROUND

Global mean near-surface temperature is an index of the temperature near the surface of the Earth averaged across its whole surface. It is estimated using air temperatures measured at weather stations at a height of around 1.5 to 2 m and sea-surface temperatures measured by ships and ocean buoys. Data are quality controlled and corrected for changes in how temperatures were measured, then gaps are filled using statistical methods. Global mean temperature can also be calculated using reanalyses, which use a weather forecasting system to combine many kinds of measurement, including satellite measurements. Reanalysis-based estimates are representative of air temperature across land and ocean.

Six datasets, including two reanalyses, were used to assess global temperature in this report (see [Datasets and methods](#)). Together they cover the period from 1850 to the present, though not every dataset covers the whole period from 1850 (Figure 2). There are minor differences between the series, and they show largely the same variations during the period in which they overlap. Differences are larger earlier in the record, leading to small differences in their assessment of long-term change (around 0.1 °C). These differences are factored into the uncertainty estimates for anomalies relative to 1850–1900.

Global mean temperature is the basis for the [Paris Agreement](#) long-term temperature goal. However, the Paris Agreement is generally considered to refer to long-term changes (decadal or longer) and not individual years. A summary of the issues can be found in the sidebar [Monitoring global temperature for the Paris Agreement](#).



Associated risks of increased global mean surface temperature and the Sustainable Development Goals

Key indicator

Ocean heat content

KEY MESSAGES

- In 2024, ocean heat content reached the highest level in the 65-year observational record, exceeding the previous record high set in 2023.
- Over the past eight years, each year has set a new record for ocean heat content.
- The rate of ocean warming over the past two decades, 2005–2024, is more than twice that observed over the period 1960–2005.

STATE OF THE INDICATOR

In 2024, observed global ocean heat content set a record, exceeding the previous record set in 2023 by 16 ± 8 ZJ (Figure 3). Over the past eight years, each year has set a new record for ocean heat content. Instrumental records start around 1960.

The rate of ocean warming over the past two decades (2005–2024), $0.99\text{--}1.07$ W m⁻² or 11.2–12.1 ZJ per year, is more than twice that observed over the period 1960–2005 ($0.27\text{--}0.34$ W m⁻² or 3.1–3.9 ZJ per year).

The latest Intergovernmental Panel on Climate Change (IPCC) report concluded that it was virtually certain that ocean heat content had increased since the 1970s and extremely likely that the main driver was human influence. Based on the datasets used here, global ocean heat content increased at a rate of 0.6 ± 0.1 W m⁻² (6.8 ZJ per year) averaged over the area of the ocean from 1971 to 2024, which is consistent with the IPCC report.⁵

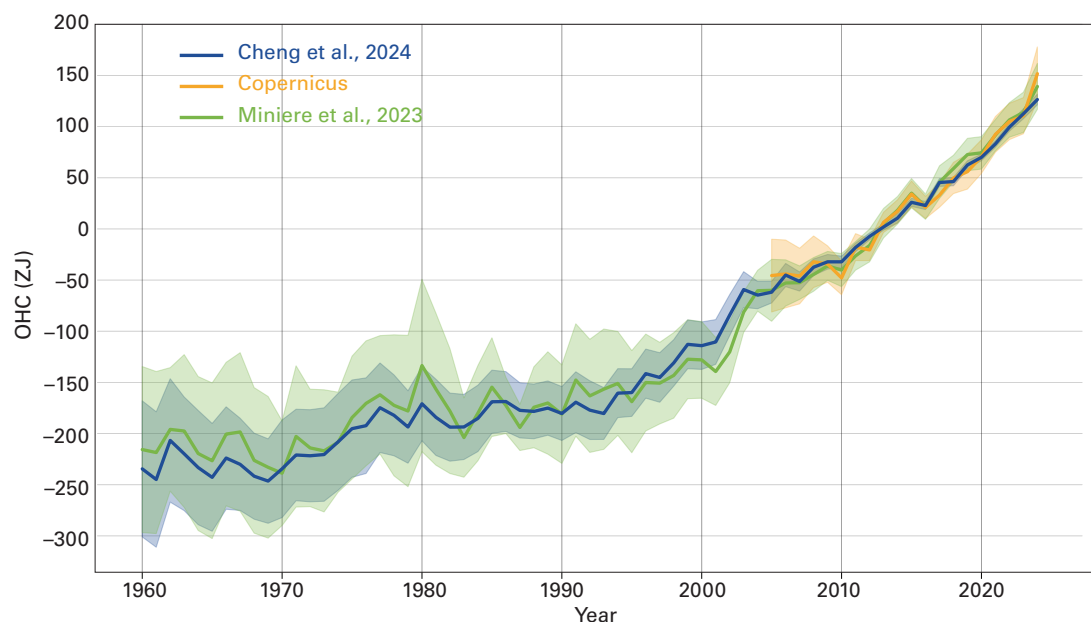


Figure 3. Annual global ocean heat content down to 2000 m depth for the period 1960–2024, in zettajoules (10^{21} J). The shaded area indicates the 2-sigma uncertainty range on each estimate. For details see [Datasets and methods](#).

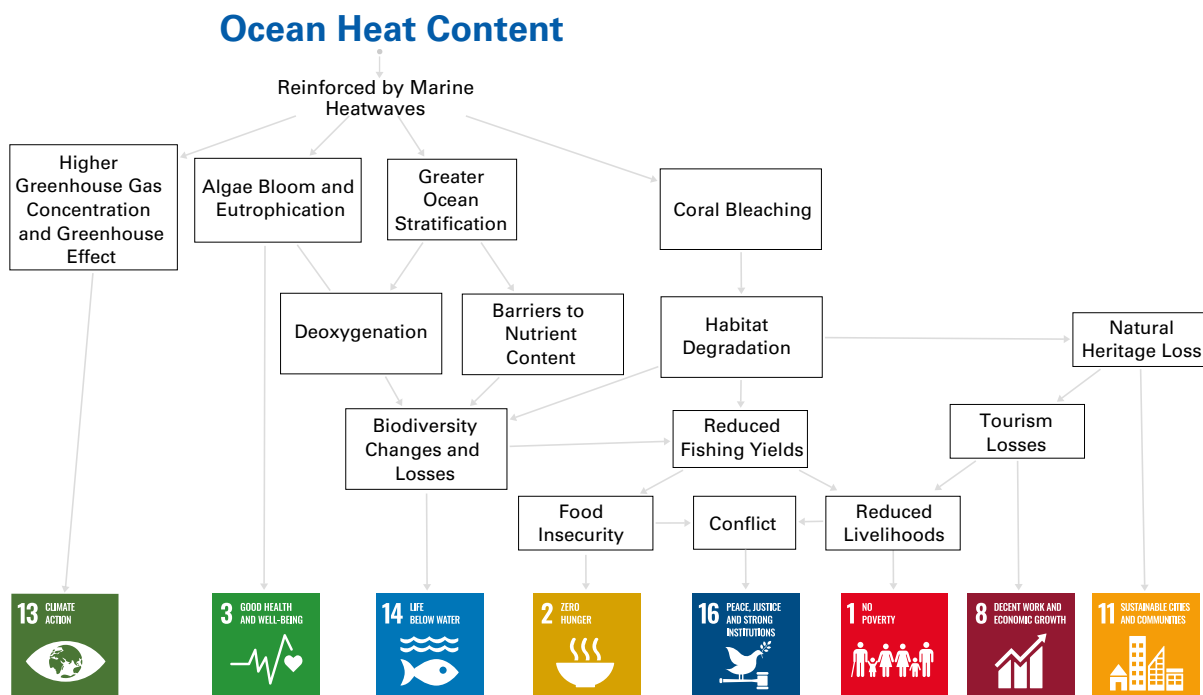
INDICATOR BACKGROUND

Observed ocean warming indicates that the Earth is currently out of energy balance. The rate of warming reveals how rapidly the Earth system is trapping surplus energy in the form of heat from climate forcings. Around 5% of that surplus energy is warming the land, 1% is warming the atmosphere, and 4% is warming and melting the cryosphere. However, the majority, around 90%, goes into warming the ocean.⁶ The indicator of ocean heat content is therefore a key indicator of climate change.

The integration of ocean temperatures from the surface to the deep ocean – typically down to 2000 m – provides a measure of ocean heat content.^{7,8} Ocean temperatures have been measured by research ships for over a century, but observations are too sparse to form a global average before 1960. Additional measurements have been made using expendable devices launched from ships since the 1970s. Since around 2005, near-global coverage down to 2000 m has been provided by autonomous Argo buoys.

The time series of ocean heat content at a global scale shows that the global ocean is clearly warming. Changes in global ocean temperature are irreversible on centennial to millennial time scales, and climate projections show that ocean warming will continue over the rest of the twenty-first century and beyond, even for low emission scenarios.⁹

Ocean warming has wide-reaching consequences, such as degradation of marine ecosystems, biodiversity loss and reduction of the ocean carbon sink. It fuels tropical and subtropical storms and exacerbates ongoing sea-ice loss in the polar regions. Ocean warming together with ice loss on land is causing sea levels to rise.¹⁰



Associated risks of increased ocean heat content and the Sustainable Development Goals

Key indicator

Global mean sea level

KEY MESSAGES

- In 2024, global mean sea level reached a record high in the satellite record (from 1993 to present).
- The rate of global mean sea-level rise in the past 10 years (2015–2024) was more than twice the rate of sea-level rise in the first decade of the satellite record (1993–2002).

STATE OF THE INDICATOR

The long-term rate of sea-level rise (Figure 4) has more than doubled since the start of the satellite record, increasing from 2.1 mm per year between 1993 and 2002 to 4.7 mm per year between 2015 and 2024. In 2024, global mean sea level reached a record high in the satellite record (from 1993 to present).

The year-to-year variability of global mean sea level around the long-term trend is correlated with the El Niño–Southern Oscillation (ENSO). The rise and fall of global mean sea level due to [El Niño and La Niña](#) arise because of the characteristic shifts in rainfall patterns that exchange water between the ocean and land as well as local changes in ocean heat content.^{11,12}

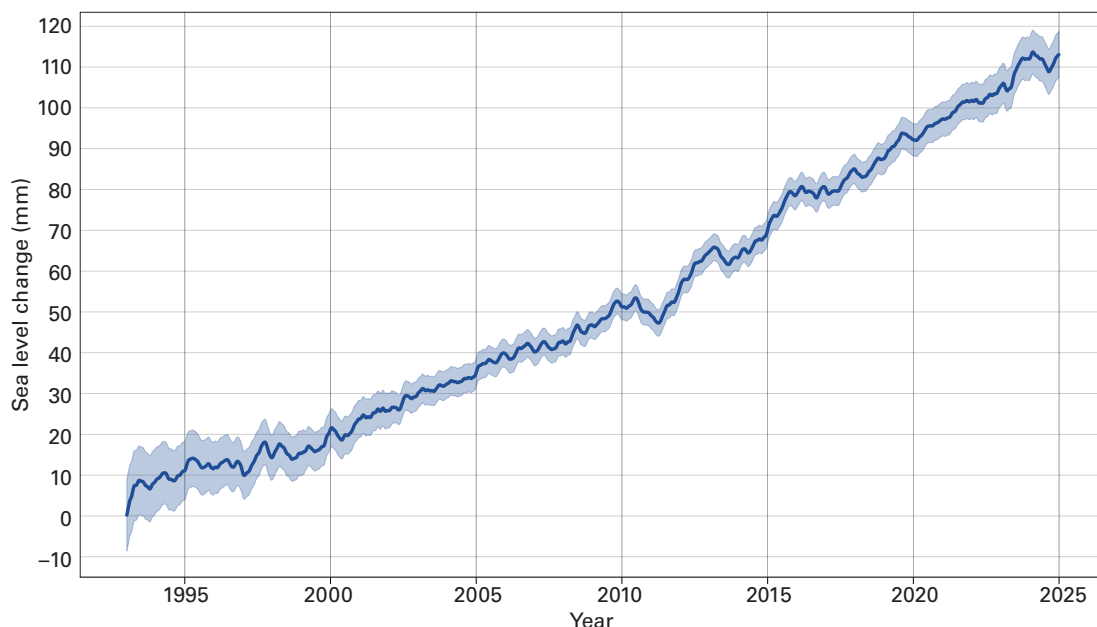


Figure 4. Seasonal global mean sea level change from 1993 shown for 1993–2024. The seasonal cycle has been removed from the data. The shaded area indicates the uncertainty.

Source: Data from AVISO CNES. For details see [Datasets and methods](#).

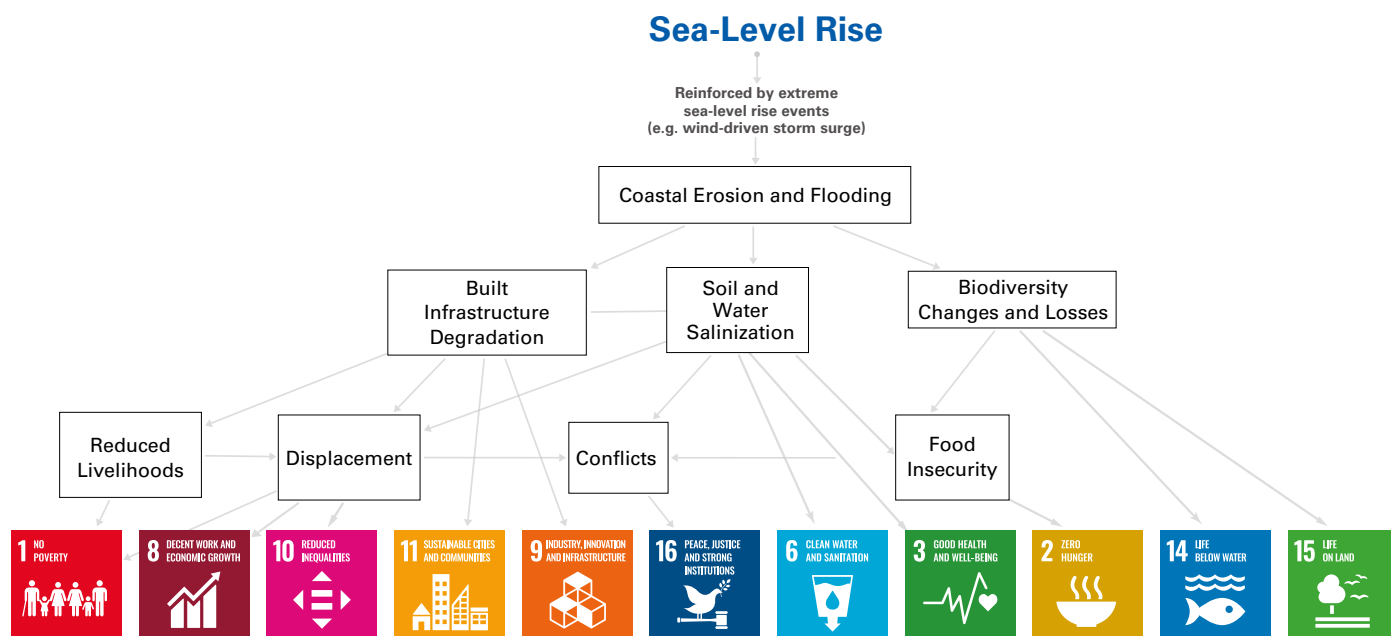
The strong 2023/2024 El Niño temporarily raised global mean sea level by several millimetres, reaching its peak in the northern hemisphere winter 2023/2024. The temporary drop in global mean sea level in the early part of 2024 corresponded to the end of the El Niño and a return to neutral conditions, though there may have been other contributory factors.

INDICATOR BACKGROUND

Global mean sea level is measured by satellites using radar altimeters that record the time taken for a radar signal to reach the sea surface and return to the satellite. Longer records of global mean sea level exist based on tide gauge measurements made along coastlines around the world since the late nineteenth century.

The warming of the ocean causes the water to expand and global mean sea level to rise. The melting of ice on the land also contributes to sea-level rise. Because warming of the oceans will continue for centuries even if emissions of greenhouse gases cease, sea level will continue to rise on the same time scale.

Changes in sea level have wide-ranging effects on coastal areas and communities. Sea-level rise will bring cascading and compounding impacts¹³ resulting in losses of coastal ecosystems and ecosystem services, groundwater salinization, flooding and damage to coastal infrastructure. These impacts cascade into risks to livelihoods, settlements, health, well-being, food and water security, as well as cultural values in the near- to long-term.



Associated risks of sea-level rise and the Sustainable Development Goals

Key indicator

Ocean pH

KEY MESSAGES

- Acidification of the ocean surface has continued over the past 39 years as shown by the steady decrease of global average ocean surface pH.
- Regionally, ocean acidification is not increasing uniformly.

STATE OF THE INDICATOR

Globally, ocean surface pH has changed at a rate of -0.017 ± 0.001 pH units per decade over the period 1985–2023 (Figure 5). The year 2023 is the latest year for which we have consolidated global figures. The decline in pH is referred to as ocean acidification. The rate of change in pH is consistent with the estimate of the latest IPCC report.¹⁴

Regionally, ocean acidification has not proceeded uniformly. The most intense decreases in regional surface pH are observed in the Indian Ocean, the Southern Ocean, the eastern equatorial Pacific Ocean, the northern tropical Pacific and some regions in the Atlantic Ocean. In these areas, which amount to 47% of the sampled global ocean, the surface of the ocean is getting more acidic at a faster rate than the global average.¹⁵

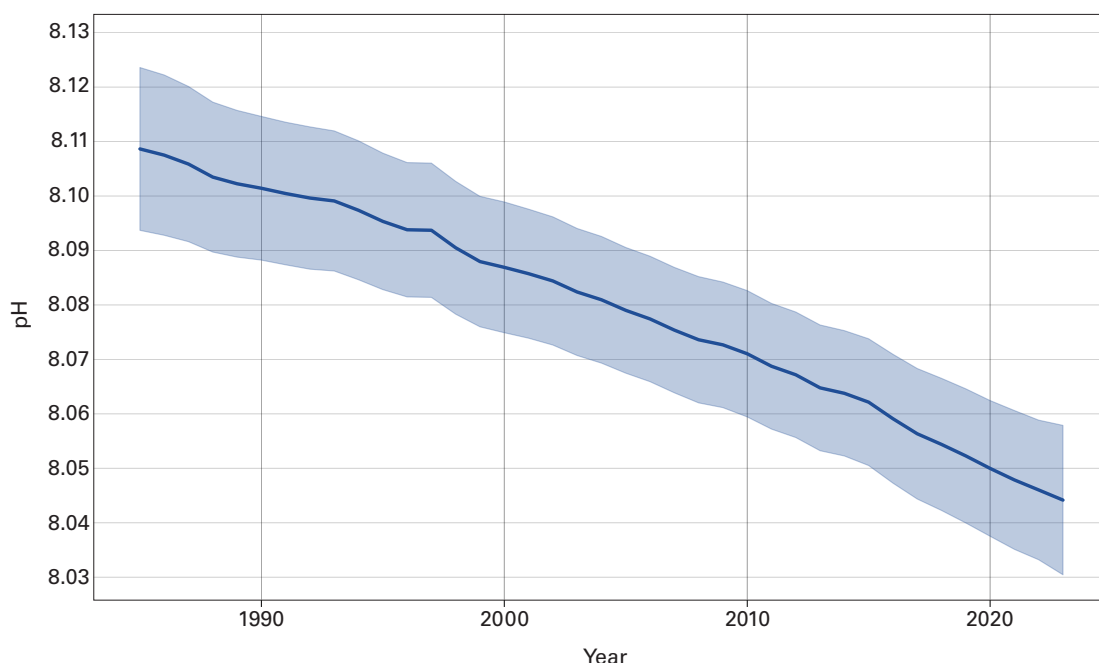


Figure 5. Annual global mean surface ocean pH 1985 to 2023. The dark line is the central estimate and the shaded area is the uncertainty range.

Source: Data from Copernicus Marine Environment Monitoring Service (CMEMS). For details see [Datasets and methods](#).

INDICATOR BACKGROUND

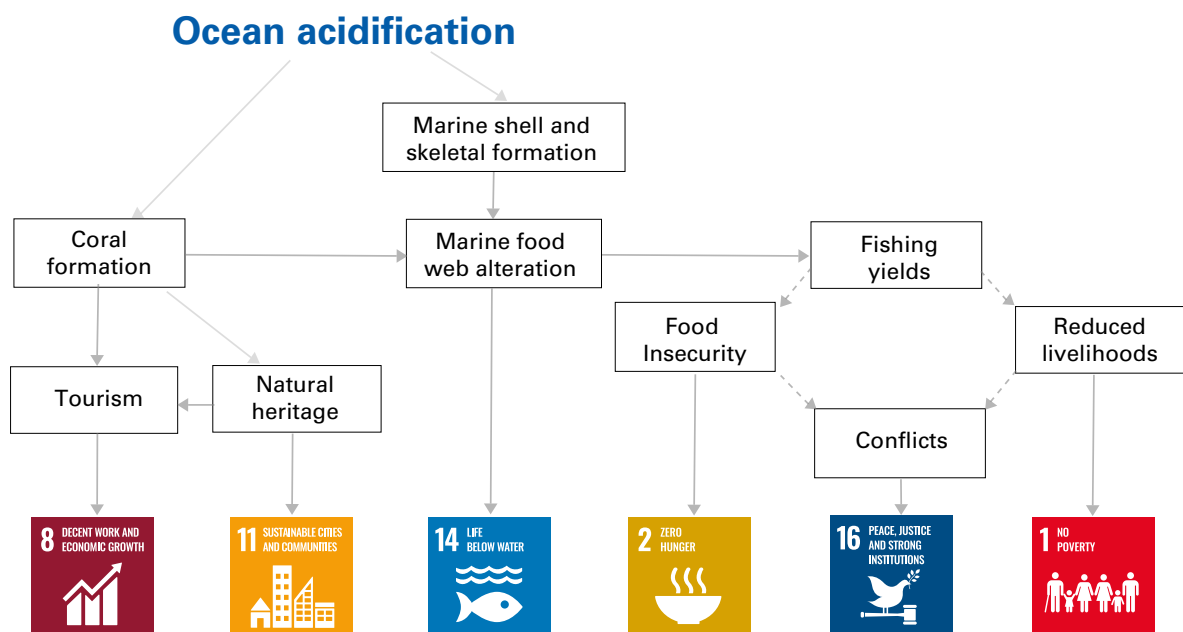
Around a quarter of the CO₂ emitted by human activities during the decade 2014–2023 was absorbed by the ocean.¹⁶ This process has caused a shift in the carbonate chemistry of the ocean, leading to a drop in pH. Ocean pH is above 7, so ocean water remains slightly alkaline, but the observed decrease in pH is referred to as ocean acidification.

Climate projections show that ocean acidification will continue to increase in the twenty-first century, at rates dependent on future emissions. Changes in deep-ocean pH are irreversible on centennial to millennial time scales.¹⁷

It is well established that ocean acidification is affecting marine life. The responses of marine organisms to the compound effects of acidification, ocean warming and deoxygenation occur at different metabolic levels for different groups, and include respiratory stress and reduction of thermal tolerance.¹⁸

The effects of ocean acidification on habitat area, biodiversity, ecosystem function and ecosystem services have already been clearly observed, and food production from shellfish aquaculture and fisheries has been adversely affected.¹⁹

Warm-water coral reefs and rocky shores dominated by immobile, calcifying organisms that produce shells and skeletons, such as corals, barnacles and mussels, are also affected by extreme temperatures and changes in pH.²⁰ The monitoring of surface ocean pH has become a focus of many international [scientific initiatives](#) and constitutes one target for [Sustainable Development Goal \(SDG\) 14](#).



Associated risks of ocean acidification and the Sustainable Development Goals

Key indicator

Glacier mass balance

KEY MESSAGES

- Glacier mass loss from 2021/2022 to 2023/2024 represents the most negative three-year glacier mass balance on record, and seven of the ten most negative annual glacier mass balances since 1950 have occurred since 2016.
- Exceptionally negative mass balances were experienced in Norway, Sweden, Svalbard and the tropical Andes.

STATE OF THE INDICATOR

Data on glacier mass balance – the amount of mass gained or lost by glaciers – for the 2023/2024 hydrological year (September–August) are not yet fully available, but preliminary observations from about 90% of the glacier data that are reported annually to the World Glacier Monitoring Service indicate that 2023/2024 was another year of extremely negative mass balance worldwide (Figure 6).

Exceptionally negative mass balances were experienced in Norway, Sweden, Svalbard and the tropical Andes. Only 2 out of the 141 glaciers reporting to date (out of a possible total of around 160) had a positive mass balance, and the composite value from the subset of 58 out of around 60 global reference glaciers indicates an average mass loss consistent with the exceptionally negative mass balance years 2021/2022 and 2022/2023, projected to be close to –1.1 metres water equivalent.

This continues a trend of accelerated glacier mass loss in the 2020s. The last three years (2021/2022–2023/2024) represent the largest negative three-year mass balance on record, and 7 of the 10 largest negative mass balance years since 1950 have occurred since 2016.

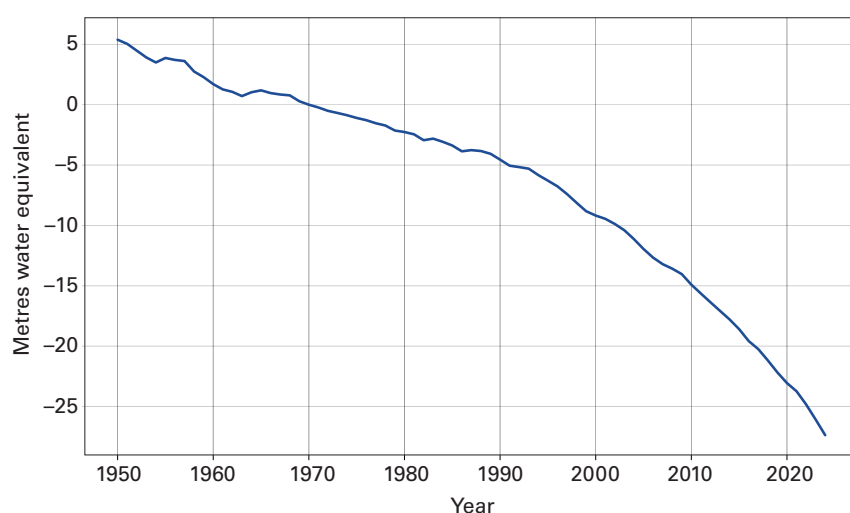


Figure 6. Cumulative annual mass balance of reference glaciers with more than 30 years of ongoing glaciological measurements. Annual mass change values are expressed in metres water equivalent, which corresponds to tonnes per square metre (1 000 kg m⁻²). The 2024 value is preliminary. For details see [Datasets and methods](#).

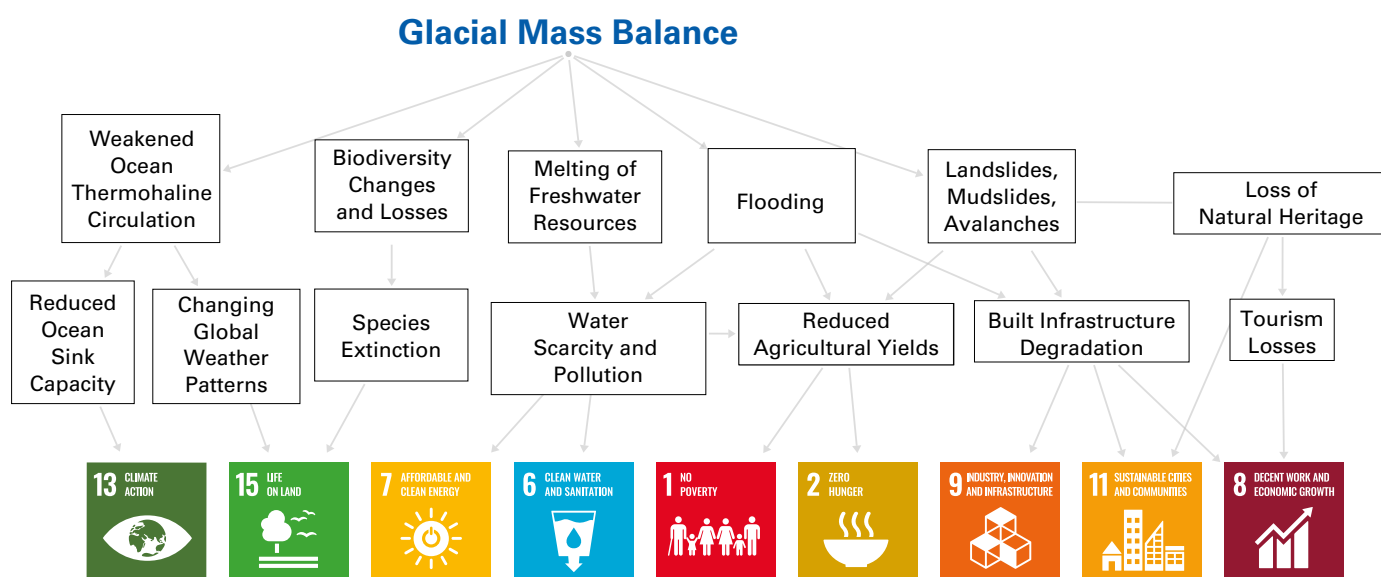
INDICATOR BACKGROUND

Glaciers are formed from snow that has compacted to form ice, which then deforms and flows downhill. Glaciers comprise two zones: an accumulation zone where accumulation of mass from snowfall exceeds ice loss, and an ablation zone where ice loss (ablation) from melting and other mechanisms exceeds accumulation. Where glaciers end in a lake or the ocean, ice loss can occur through melting where the ice meets the water, and via calving when chunks of the glacier break off.

Glacier mass balance – the amount of mass gained or lost by the glacier – is commonly expressed as the annual thickness change averaged over the glacier area, expressed in metres water equivalent. One metre water equivalent is approximately the same as one tonne per square metre. Ice loss from glaciers contributed around 21% of the total sea-level rise over the period 1993–2018, around half the contribution from expansion due to ocean warming (42%) but larger than contributions from melting of the ice sheets in Greenland (15%) and Antarctica (8%).²¹

The mass balances of individual glaciers are affected by changes in temperature, precipitation, humidity and cloudiness. The IPCC Sixth Assessment Report (AR6) concluded that human influence is very likely the main driver of the global retreat of glaciers since the 1990s, stating that “[t]he global nature of glacier retreat since the 1950s, with almost all of the world’s glaciers retreating synchronously, is unprecedented in at least the last 2 000 years (*medium confidence*)”.²²

Melt rates are also strongly affected by the glacier albedo, the fraction of sunlight that is reflected by the glacier surface. Exposed glacier ice is darker and therefore has a lower albedo than the seasonal snowpack; it is also sensitive to darkening from mineral dust, black carbon, algal activity and fallout from forest fires. Reduced snow cover, long melt seasons and wildfire activity all concentrate darker material on the glacier surface, decreasing its albedo and thereby increasing the rate of melting.



Associated risks of declining glacier mass balance and the Sustainable Development Goals

Key indicator

Sea-ice extent

- The minimum daily extent of Arctic sea-ice in 2024 was the seventh lowest in the observed record (1979 to present).
- The 18 lowest Arctic sea-ice extent minima in the satellite record all occurred in the past 18 years.
- The annual minimum and maximum of Antarctic sea-ice extent were each the second lowest in the observed record (1979 to present).

STATE OF THE INDICATOR

The extents of sea-ice in the Antarctic and Arctic regions in 2024 were both below their respective 1991–2020 averages throughout the annual cycle (Figure 7).

The minimum daily extent of sea-ice in the Arctic in 2024 was 4.28 million km² on 11 September, which is the seventh lowest extent in the 46-year satellite record. This is 1.17 million km² below the average minimum daily extent from 1991–2020. The 18 lowest minima in the satellite record all occurred in the past 18 years.

The minimum daily extent of sea-ice in the Antarctic region in 2024 was 1.99 million km² on 20 February, which tied for the second lowest minimum in the satellite era²³ and marked the third consecutive year that minimum Antarctic sea-ice extent dropped below 2 million km². These are the three lowest Antarctic ice minima in the satellite record.

Antarctic ice extent remained below the 1991–2020 average throughout the year and reached its annual maximum daily extent of 17.16 million km² around 19 September. Six days of missing

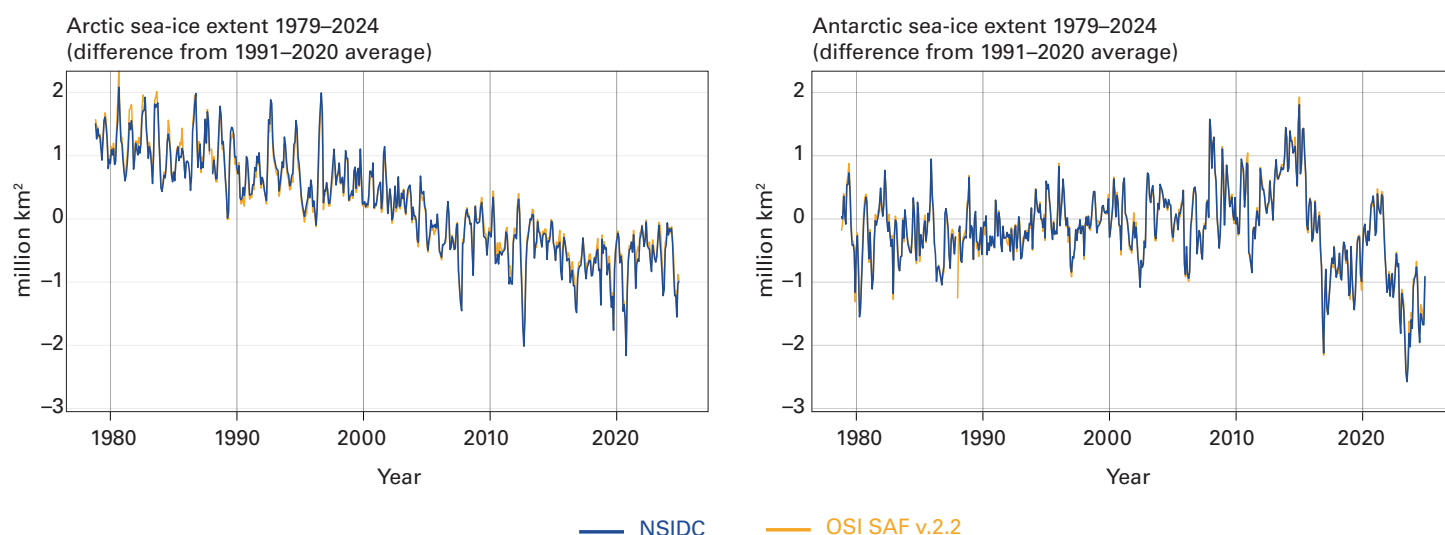


Figure 7. Monthly Arctic (left) and Antarctic (right) sea-ice extent anomalies (difference from the 1991–2020 average) in millions of square kilometres from 1979 to 2024

Source: Data from NSIDC and OSI SAF. For details see [Datasets and methods](#).

data near the maximum mean there is some uncertainty in the exact extent and date. The observed maximum was 1.55 million km² below the average Antarctic maximum daily ice extent from 1991–2020 and is the second lowest maximum ice extent on record; only in 2023 was it lower. The year ended with extents slightly below the 1991–2020 average.

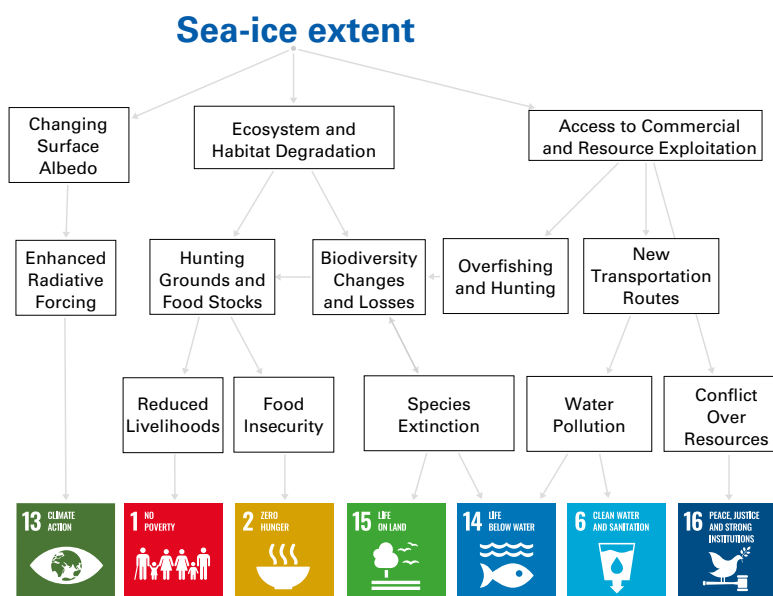
INDICATOR BACKGROUND

Sea ice is frozen sea water that floats on the surface of the ocean. Sea-ice cover expands in Earth's polar regions each autumn and winter, as ocean water freezes in response to cooling of the atmosphere and ocean. Summer warming melts much of this seasonal ice, with annual sea ice minima in each hemisphere typically recorded in late summer or early autumn (September in the northern hemisphere, February in the southern hemisphere). Changes in sea-ice cover can affect ocean circulation, atmospheric dynamics and surface heating.

Sea-ice extent is defined as the area of the ocean with at least 15% ice cover. This is a dynamic quantity, which changes in response to both thermodynamic growth (freezing) and decay (melting) as well as when the ice pack moves with winds and ocean currents. Sea-ice extent and sea-ice cover are mapped using microwave satellite imagery.

Long-term changes in Arctic sea-ice extent have been seen throughout the seasonal cycle. The downward trend in the minimum Arctic sea-ice extent from 1979 to 2024 is around 14% of the 1991–2020 average per decade, equivalent to a sea-ice loss of 77 000 km² per year.

Until 2015, Antarctic maximum sea-ice extent had a small but positive long-term trend. However, after recent low extents, that is no longer the case. While the last three years have had anomalously low Antarctic ice cover, it remains to be seen if there has been a regime shift in Antarctic sea ice.^{24,25}



Associated risks of decreasing sea-ice extent and the Sustainable Development Goals

Climate driver – El Niño–Southern Oscillation

KEY MESSAGES

- The strong 2023/2024 El Niño followed three consecutive years of La Niña from late 2020 to early 2023.
- El Niño conditions were established by mid-2023, became strong by the end of 2023 and dissipated by the second quarter of 2024.

STATE OF EL NINO-SOUTHERN OSCILLATION (ENSO)

Following a prolonged La Niña, which lasted from 2020 to early 2023, an El Niño became well-established by September 2023. The event peaked during November 2023–January 2024 when the Oceanic Niño Index reached 2.0 °C, the highest peak since the 2015/2016 El Niño and the fifth highest peak since 1950, the start of the timeseries.

From January 2024, sea-surface temperature anomalies in the eastern tropical Pacific began to decrease, returning to ENSO-neutral conditions around June. Neutral or weakly La Niña conditions remained at the end of 2024.

Global temperatures in 2023 and 2024 were higher than the preceding years, which is typical when El Niño conditions occur. Every month of 2024 saw record or near-record warmth, and the annual mean temperature for the year was a record high. However, other factors were likely at play too (see sidebar on [Global mean surface temperature anomalies in 2023/2024](#)). Some of the rainfall patterns in 2024, such as the dry conditions over northern South America and Southern Africa, were characteristic of El Niño (see Figure 8).

Typical impacts of El Niño on precipitation January–June

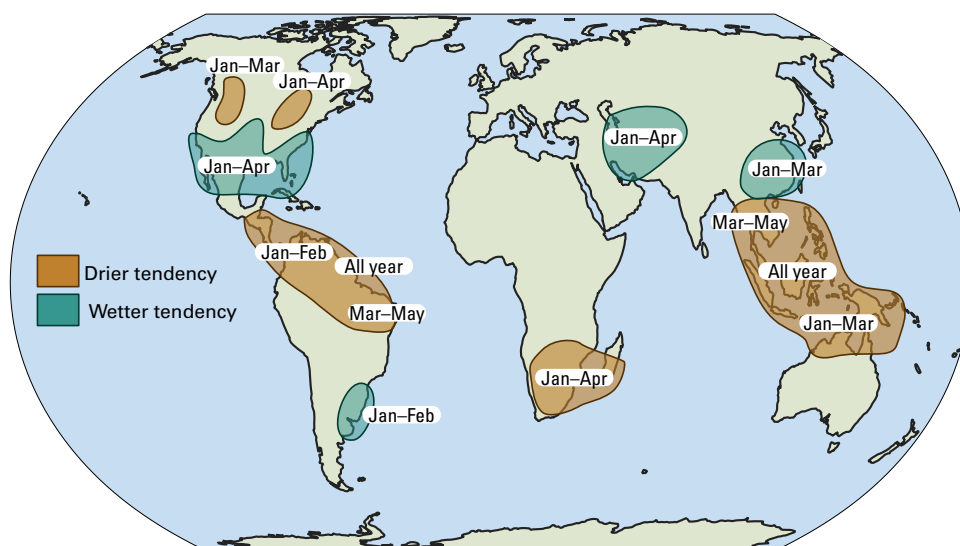


Figure 8. Typical El Niño seasonal precipitation effects for January to June based on various sources, see [Datasets and methods](#). Note this is not a forecast; it is based on historical associations between El Niño and precipitation.

The transition from El Niño to neutral conditions during 2024 was also likely associated with a temporary drop in global mean sea level.

DRIVER BACKGROUND

The El Niño–Southern Oscillation (ENSO) is one of the most important drivers of year-to-year and seasonal variability in weather patterns worldwide. It is linked to changes in the occurrence and distribution of hazards such as heavy rains, floods, and drought, heatwaves, and cold spells.

El Niño is characterized by higher-than-average sea-surface temperatures in the eastern tropical Pacific and a weakening of the trade winds in the region. The weakened trade winds reduce upwelling of cooler waters along the coast of South America, which in turn leads to higher sea-surface temperatures.

La Niña, which is characterized by below-average sea-surface temperatures in the central and eastern tropical Pacific and a strengthening of the trade winds, has effects that are generally the opposite of those of El Niño.

El Niño typically has a temporary warming influence on global average temperature, and La Niña generally has a temporary cooling influence. The greatest warming or cooling effects usually occur two to three months following the event peak because it takes time for the excess heating or cooling in the ocean to spread to and through the atmosphere.

El Niño and La Niña have an influence on regional rainfall patterns around the world, which can vary depending on the strength and timing of the event and other concurrent meteorological factors. Figure 8 shows some typical precipitation anomalies that are favoured by El Niño conditions. However, each El Niño is different, and other factors also influence rainfall.

The change in rainfall patterns can also affect sea level, with higher global mean sea level during El Niño events and lower global mean sea levels during La Niña events.

Please refer to the sections on [Precipitation](#) and [High-impact events](#) for more details of the events in 2024. Details on the evolution of ENSO can be found in the [WMO El Niño/La Niña updates](#).

Global patterns of temperature and precipitation

TEMPERATURE

Most land areas were warmer than the long-term average (1991–2020) in 2024, with limited areas of below-average temperatures around Iceland, parts of Antarctica and the southern tip of South America (Figure 9). Record or near-record high annual mean temperatures were observed across large areas of the tropics from South and Central America east to the western Pacific. Other land areas outside of the tropics also experienced exceptionally high annual temperatures, including eastern North America, North Africa and Europe, and southern and eastern Asia.

Sea-surface temperatures reached record highs in the tropical and North Atlantic, tropical Indian Ocean, parts of the western Pacific and parts of the Southern Ocean. Despite El Niño conditions at the start of the year, cooler than average waters were observed along the west coast of South America, with above-average temperatures more evident further west along the equator.

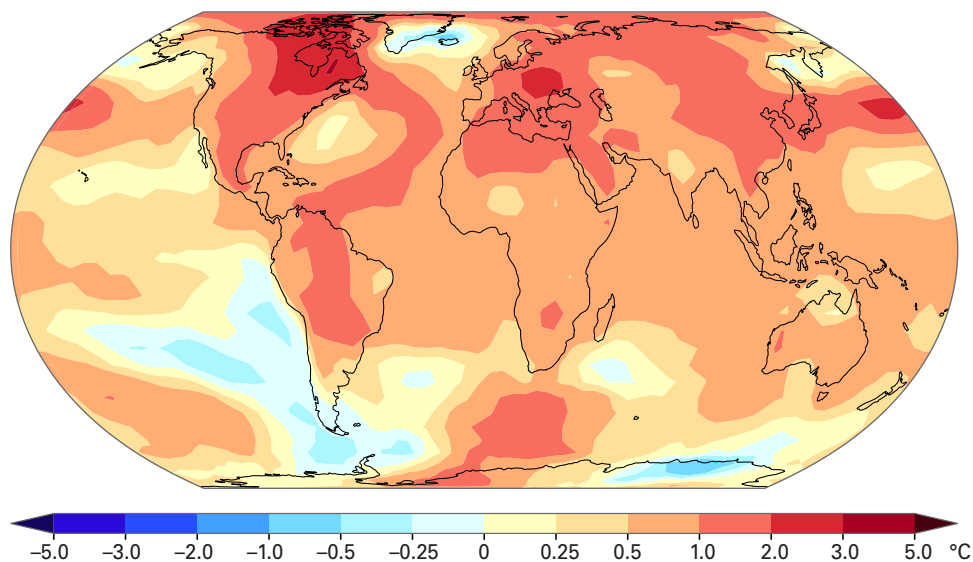


Figure 9. Annual average temperature anomalies relative to the 1991–2020 average. The values shown are the median of six global temperature datasets.

Source: Data from six global temperature datasets. For details see [Datasets and methods](#).

PRECIPITATION

In 2024, drier than average (1991–2020) conditions were observed (Figure 10) over much of Southern Africa, some locations in coastal West Africa as well as along the North African coast. Large parts of South America, from the Amazon lowlands and northern Andes to the Pantanal wetlands, were also drier than normal. North-western Mexico, some islands in the Caribbean and parts of northern North America had unusually low precipitation totals. Areas along Australia’s southern coast, the northern parts of New Zealand, New Caledonia and central and eastern islands in Polynesia had lower precipitation amounts than normal. Also, South and South-east Europe were drier than usual.

Parts of the Sahel region and parts of Central and southern East Africa were wetter than normal. Central and western Europe were also wetter than the long-term average. The western islands of Polynesia, northern Melanesia as well as southern New Zealand and parts of eastern and northern Australia were wetter than average. The Canadian Archipelago and some locations around the Gulf of Mexico were wetter than usual. Higher-than-normal precipitation totals were observed in large parts of North-east, East and Central Asia and to a smaller extent also in South-east, South and South-west Asia.

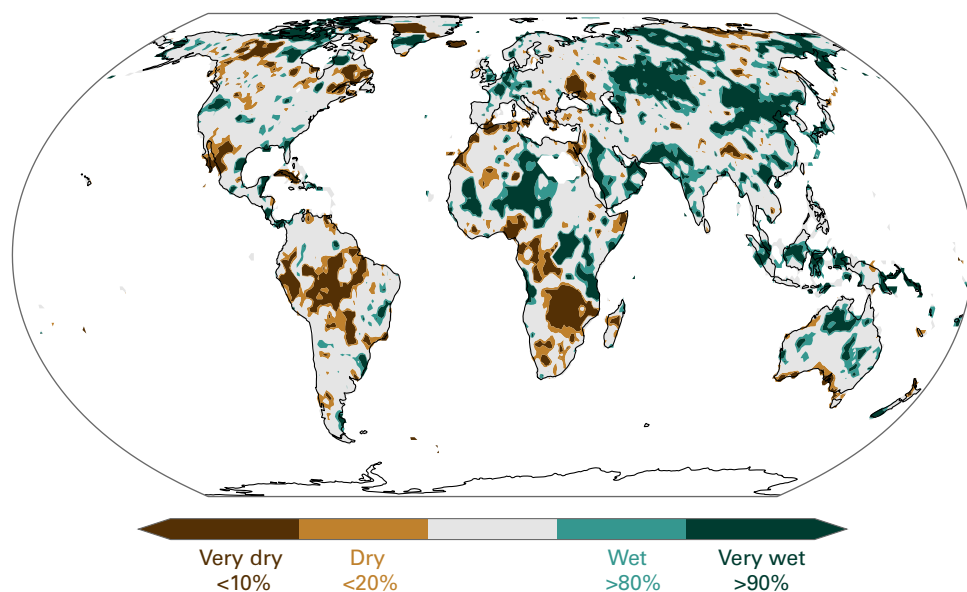


Figure 10. Annual precipitation 2024 expressed as percentiles of the 1991–2020 distribution. Brown areas are unusually dry. Green areas are unusually wet.

Source: Data from Global Precipitation Climatology Centre (GPCC).

High-impact events

This section describes some notable high-impact weather and climate events from 2024 and their socioeconomic impacts. For a more detailed list, please see the [supplement on extremes](#) and the [interactive extremes map](#).

Extreme weather events in 2024 led to the highest number of new displacements recorded in a year since 2008. New, onward and protracted displacements affected significant numbers of people in fragile and conflict affected contexts. Alongside the destruction of homes, critical infrastructure, forests, farmland and biodiversity, such extreme weather events undermine resilience and pose significant risks to people on the move and those already living in displacement. The compounded effects of various shocks, such as intensifying conflict, drought and high domestic food prices, drove worsening food crises in 18 countries globally by mid-2024.²⁶ Eight countries had at least 1 million more people facing acute food insecurity in 2024 than during the 2023 annual maximum. The reduced global cereal harvest is the result of widespread drought, linked in some regions, such as Southern Africa, to the El Niño conditions.

Tropical cyclones were responsible for many of the highest-impact events of 2024. Typhoon *Yagi* in early September made landfall in northern Viet Nam after first crossing the Philippines and the southernmost parts of China. Casualties²⁷ and displacements were reported in Viet Nam, the Philippines, the Lao People's Democratic Republic, Thailand and Myanmar.²⁸ Significant wind damage occurred in China and the Philippines.

In the United States of America, Hurricanes *Helene* in late September and *Milton* in October both made landfall on the west coast of Florida as major hurricanes. Both had major impacts at landfall, and *Helene* went on to produce exceptional rainfall and extreme flooding in the interior south-east of the United States, especially western North Carolina. Both hurricanes had economic impacts of tens of billions of dollars. Over 200 deaths²⁹ were associated with *Helene*, the most associated with a mainland United States hurricane since *Katrina* in 2005.

In the southern hemisphere in December, Tropical Cyclone *Chido* crossed the French Indian Ocean department of Mayotte before making landfall in Mozambique and moving onwards to Malawi, with major damage and significant loss of life in all three. In Mozambique, Cyclone *Chido* displaced around 100 000 people,³⁰ destroyed homes, and severely damaged roads and communication networks, hampering relief efforts in areas already hosting large numbers of displaced people. Similarly, vulnerable communities in Mayotte faced increased risks because of the destruction brought by Cyclone *Chido*.^{31,32,33}

Afghanistan and neighbouring areas of Pakistan and the Islamic Republic of Iran suffered a succession of disasters in late winter and spring, with abnormal cold and highland snow in late February and early March 2024, then several flood events over the following months, the worst of which affected Afghanistan between 10 and 17 May. Around 35 000 ha of cropland were flooded on 30 May.³⁴ Several hundred deaths were reported in the flooding,³⁵ and the cold wave also resulted in significant loss of life.

From mid-year onward, an abnormally active monsoon brought major flooding to many parts of the Sahel in Africa. Almost every country in the region reported significant impacts, with flooding affecting large areas of cropland³⁶ and leading to a significant number of deaths. Between March and May, floods mostly impacted^{37,38,39} equatorial East Africa, with major loss of life in countries such as Kenya and Tanzania as well as displacements, destruction of croplands and loss of livestock. Lake Victoria reached record high water levels, with resultant downstream flooding badly affecting South Sudan later in the year.

In contrast, dry conditions in what is usually the wet season in late 2023 and early 2024 resulted in significant drought in north-western Africa and many parts of interior Southern Africa,⁴⁰ particularly Zimbabwe, Zambia,⁴¹ Botswana and Namibia. The severe drought led to significant impacts on agriculture and hydroelectric production.

Chile suffered destructive wildfires early in the year. A fire around the city of Viña del Mar on 2–3 February resulted in over 300 deaths⁴² and damages to several thousand properties, amongst the worst losses in a wildfire anywhere in the world this century. It was also a very active wildfire season in Canada,⁴³ where wildfire carbon emissions were the second highest on record (2003–present),⁴⁴ and the area burned was one of the five highest on record (1983–present). The western United States also had an active wildfire season. In total, over 300 000 displacements were reported across both countries.⁴⁵

Drought affected many parts of the Americas; severe drought in Mexico and parts of Central America in 2023 persisted into the early months of 2024,⁴⁶ while there was also significant drought in much of interior South America. The Rio Negro at Manaus and the Paraguay River at Asunción both reached record low levels, and the number of wildfires in the Brazilian Amazon was the largest since 2010.

An exception to the generally dry conditions in South America was the flooding in early May in Rio Grande do Sul state of southern Brazil. Persistent heavy rainfall resulted in flooding which inundated large parts of the city of Porto Alegre and many surrounding areas with significant effects⁴⁷ on agriculture and fisheries as well as over 200 deaths.⁴⁸

Extreme rainfall resulted in severe flash flooding in the Valencia region of Spain on 29 October, associated with an upper-level cold pool over southern Spain. Turis in the west of Valencia reported 185 mm of rain in one hour, a Spanish national record. In six hours, 621 mm of rain fell, and 772 mm was recorded in 24 hours. The rainfall led to exceptional flooding downstream, particularly affecting the southern part of the Valencia metropolitan area. Over 200 deaths⁴⁹ and severe damages were reported in the Valencian Community and surrounding areas.

There were numerous significant heatwaves in 2024, with many featuring prolonged periods of heat and records broken at many stations over large areas. According to the WMO *2023 State of Climate Services* report,⁵⁰ the impacts of extreme heat and heatwaves are underestimated, and heat-related mortality could be many times higher than current estimates.

During the northern hemisphere summer, areas particularly affected by heatwaves included East Asia, South-east Europe, the Mediterranean and Middle East, and the south-western United States. This followed record-breaking heat in many parts of the northern hemisphere tropics during the pre-monsoon period from late March to May, including South-east Asia, West Africa and the Sahel, and Central America, as well as northern India.

Amongst the most significant events was the June heatwave in Saudi Arabia, when temperatures near Mecca reached 50 °C during the Hajj pilgrimage. Many casualties were reported during the pilgrimage, the large majority of which were partially or wholly attributable to the extreme heat.

Early warning systems have proved to be efficient systems that governments can use to move communities out of harm's way before a disaster or manage the event in situ. Reliable data and effective disaster risk reduction policies are crucial to saving lives. Disaggregated data – showing the frequency, triggers and sequence of displacement – can help response and development planners mitigate impacts on displaced people and host communities.

Monitoring global temperature for the Paris Agreement

Individual years with annual global mean temperatures exceeding 1.5 °C above the 1850–1900 average do not mean that the goal of “pursuing efforts to limit the temperature increase to 1.5 °C above pre-industrial levels” as stated in the Paris Agreement is out of reach.

Global temperature does not increase smoothly from one year to the next (Figure 2). In addition to the long-term warming principally driven by greenhouse gas emissions (Figure 1), there is considerable year-to-year natural climate variability caused by phenomena such as El Niño and La Niña, volcanic activity and changes in ocean circulation.

The IPCC defines climate change as a change in the state of the climate that persists for an extended period, typically decades or longer. The exceedance of the 1.5 °C and 2.0 °C warming levels referred to in the Paris Agreement should therefore be similarly understood as an exceedance over an extended period, although the Agreement itself does not provide a specific definition.

As the world continues to warm there is a policy-driven need to clearly define, measure and monitor warming relative to the goal specified in the Paris Agreement. The latest IPCC assessment report defines future global warming levels in terms of 20-year averages relative to the average for 1850–1900. The year of exceedance of a particular level, such as 1.5 °C, is the midpoint of the 20-year period that first exceeded that level.

By this definition, 1.5 °C of warming would only be confirmed once the observed temperature has reached that level over a 20-year period, 10 years after the year of exceedance. Thus, there would be a 10-year delay in recognizing and reacting to exceedance of the long-term temperature goal. Even taking a shorter average of 10 years, as done in IPCC AR6 and the First Global Stocktake, would result in a 5-year delay.

Several approaches are under consideration by WMO and the international scientific community to enable more timely reporting. These approaches fall broadly into three categories. The first combines the most recent 10 years of observed historical temperature with climate model projections for the next 10 years.⁵¹ The second fits a trend or function to the historical data to better estimate where the long-term warming is today.⁵² The third estimates the human factor in the historical change by estimating the underlying warming resulting from historical changes in key human drivers of the climate system such as greenhouse gases (update of Forster et al., 2024⁵³).

The best estimates of current global warming from these three approaches are between 1.34 °C and 1.41 °C compared to the 1850–1900 baseline; however, given the uncertainty ranges, the possibility that we have already exceeded 1.5 °C cannot be ruled out (Figure 11). To further explore the issue, WMO has convened a team of international experts to define a suitable metric, and propose a method for monitoring it aligned with IPCC approaches to ensure consistent, reliable tracking of long-term global temperature changes.

Ultimately, it is essential to recognize that, regardless of the methodology used to track global temperature, every fraction of a degree of warming matters. Whether it is at a level below or above 1.5 °C of warming, every additional increment of global warming leads to changes in extremes and risks becoming larger.

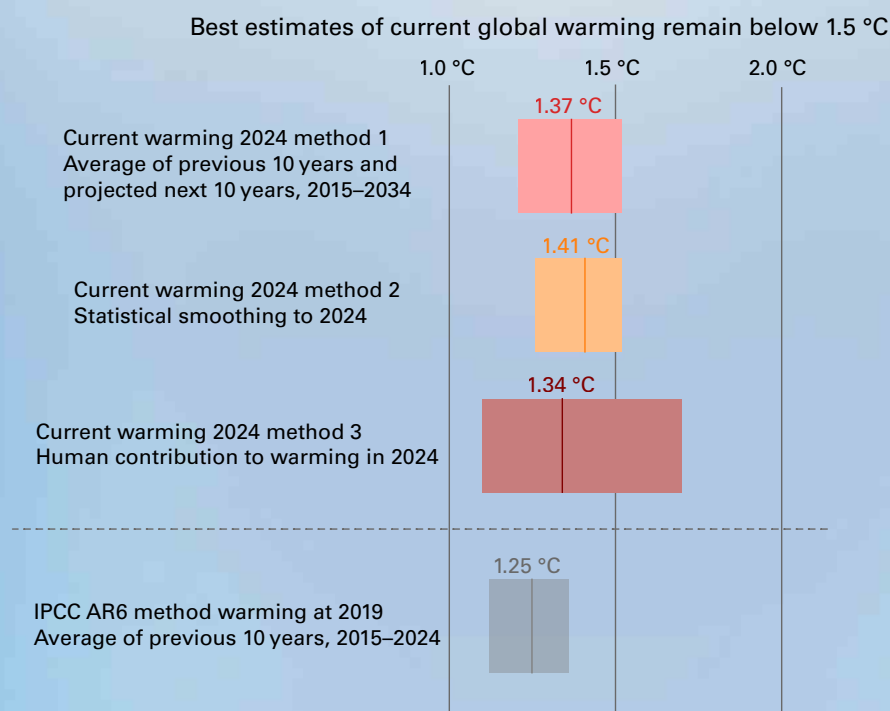


Figure 11. Three methods for establishing an up-to-date estimate of current global warming as of 2024, compared with the IPCC AR6 method, which uses averages over the previous 10 years and is representative of warming to 2019. The best estimate resulting from each method is shown as a dark vertical line, and the uncertainty range is shown by the shaded area.

Global mean surface temperature anomalies in 2023/2024: Towards understanding the influencing factors

This section explores open science questions, and research on the topic is still evolving.

The records in global mean surface temperature set in 2023 and 2024 occurred in the context of rising temperatures driven by a continued increase in emissions of anthropogenic greenhouse gases (GHGs). However, despite the transition from La Niña to El Niño, the specific magnitudes of the anomaly in 2023 (and to a lesser extent that in 2024) drew attention for being at the edge of, or outside of, ranges from [individual forecasts](#). According to some analyses (for example, that of Rantanen and Laaksonen⁵⁴), they were at the far end of what has been expected from climate model estimates of trends plus internal variability.

A number of additional factors might help explain these records: a faster-than-expected onset of Solar Cycle 25, the developing impacts of the International Maritime Organization (IMO) rules on shipping fuel sulfur content that came into force in January 2020, the eruption of Hunga Tonga–Hunga Ha’apai (HTHH) in January 2022, and decadal decreases in aerosol emissions from East Asia (Figure 12). Anomalous patterns of internal variability in Saharan dust over the Atlantic and/or Antarctic sea-ice extents may also have played a role.

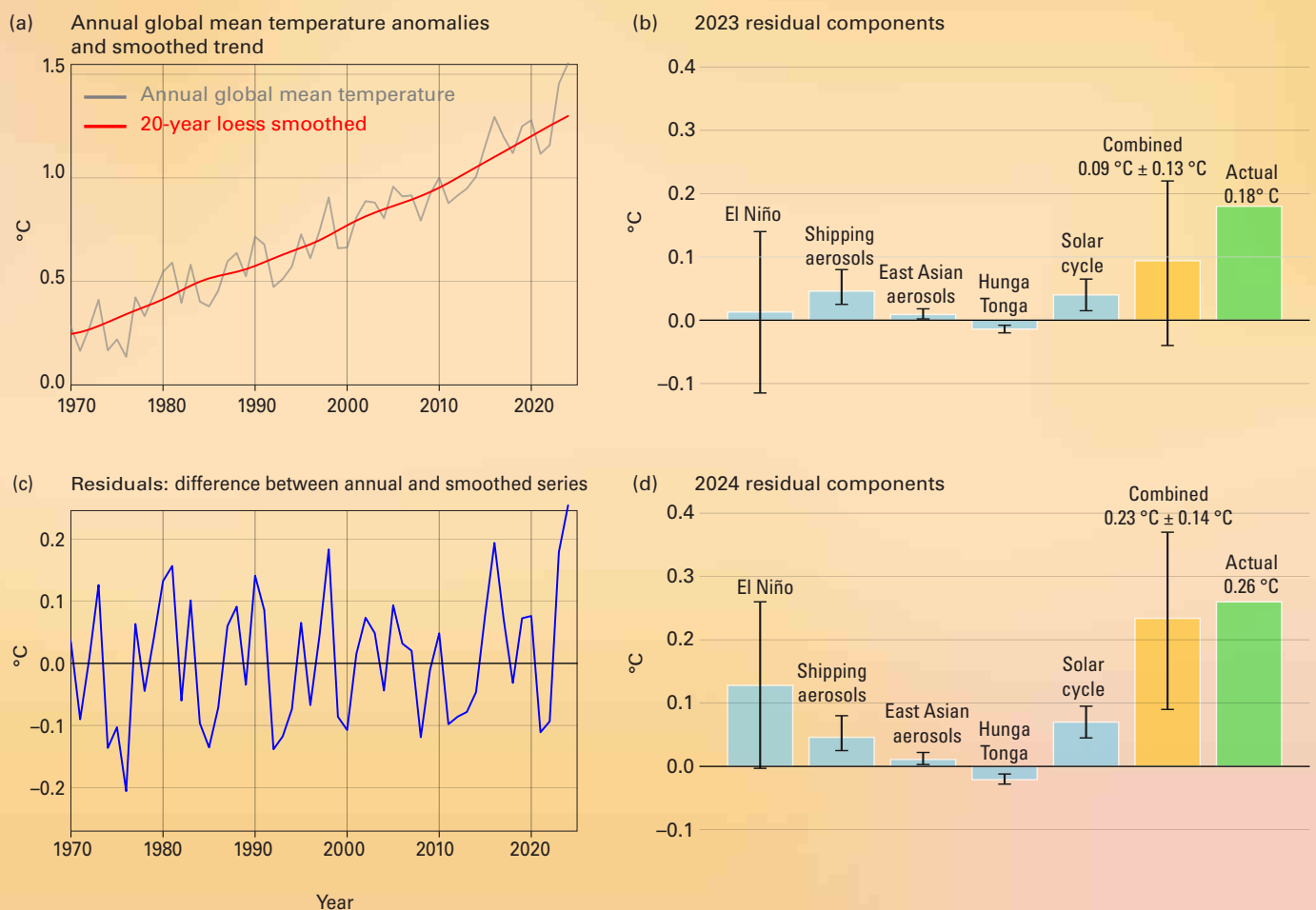


Figure 12. (a) Annual global mean temperature. Estimates of relative temperature residuals for (b) 2023 and (d) 2024 attributable to ENSO and four distinct forcings that were not (or were only partially) predicted. The (c) residuals are calculated by taking the difference between the annual global mean temperatures and the 20-year loess smoothed curve fitted to the data through to 2022. Uncertainties are nominally the 95% confidence level.

Determining the impact of each of these effects on global temperatures has been complicated by the time needed to assemble estimates of historical emissions; hence, no fully comprehensive syntheses have yet been published. Nonetheless, a rough estimate can be made by combining the results of recent studies. For details of the methods, see [Data sets and methods](#).

Here, we focus on “residuals” (Figure 12c), that is the differences from a smoothly rising trend calculated over the period through to the end of 2022. The residuals for 2023 and 2024 are 0.18 °C and 0.26 °C, respectively. We estimate the contribution to the residuals in 2023 and 2024 from five quantifiable external drivers (GHGs, shipping aerosols, East Asian aerosols, the HTHH volcanic eruption and the solar cycle), and additionally include an estimate for the impact of ENSO, which went from a multi-year La Niña at the beginning of 2023 to El Niño at the end of 2023 and back to neutral or mild La Niña conditions at the end of 2024. The impact of GHGs on the residuals in these two years is small (<0.01 °C), as changes from GHGs are represented in the smoothly rising trend line. They dominate the anomaly with respect to the pre-industrial period.

In total, there is an additional radiative forcing from these drivers in recent years of $\sim 0.14 \text{ W m}^{-2}$, and the consequent warming ($\sim 0.1 \text{ °C}$) combined with the effect of ENSO come close to explaining the residuals (taking into account the uncertainties), although this is more true for 2024 than for 2023 (Figure 12(b) and (d)). The warming contribution of shipping and East Asian aerosol reductions are likely to persist, contributing to a slight jump in long-term temperatures not fully accounted for in existing projections.

Fuller analyses of these factors and the role of internal variability will require coordinated Earth system model experiments, which are currently underway. The sensitivity of the attribution to the strength of each model’s cloud feedbacks, aerosol–cloud interactions, etc. remains to be seen. We stress that this is a preliminary estimate that will be refined as more sophisticated studies are undertaken.

Datasets and methods

BASELINES

Baselines are periods of time, usually spanning three decades or more, that are used as a fixed benchmark against which current, and future, conditions can be compared. For scientific, policy and practical reasons, several different baselines are used in the present publication, and these are specified in the text and figures. Where possible, the most recent WMO climatological standard normal, 1991–2020, is used as the baseline for consistent reporting.

For some indicators, however, it is not possible to use the standard normal owing to a lack of measurements during the early part of the period. There are also two specific exceptions. First, for the global mean temperature time series – and only for the global mean series – a reference period of 1850–1900 is used. This is the baseline used by IPCC Working Group I (WG I) in its contribution to AR6 as a reference period for pre-industrial conditions and is relevant for understanding progress in the context of the Paris Agreement and other considerations in the United Nations Framework Convention on Climate Change. Second, greenhouse gas concentrations can be estimated much further back in time than 1850 using gas bubbles trapped in ice cores. The year 1750 is used in this report to represent pre-industrial greenhouse gas concentrations in line with IPCC AR6 WG I.

GREENHOUSE GAS DATA

Estimated concentrations from the year 1750 are used to represent pre-industrial conditions. Calculations assume a pre-industrial mole fraction of 278.3 ppm for CO₂, 729.2 ppb for CH₄ and 270.1 ppb for N₂O.⁵⁵

Data and analysis from:

World Data Centre for Greenhouse Gases operated by the Japan Meteorological Agency, <https://gaw.kishou.go.jp/>

World Meteorological Organization (WMO). *WMO Greenhouse Gas Bulletin – No. 20: The State of Greenhouse Gases in the Atmosphere Based on Global Observations through 2023*. Geneva, 2024.

GLOBAL TEMPERATURE DATA

GLOBAL MEAN TEMPERATURE SERIES

The method for calculating global mean near-surface temperature anomalies relative to an 1850–1900 baseline is based on the assessment of long-term change and its uncertainty in IPCC AR6 WG I. In 2021, IPCC AR6 WG I assessed change from 1850–1900 to other periods based on an average of four datasets – HadCRUT5, Berkeley Earth, NOAA Interim and Kadow et al. (2020) – which start in 1850 and are globally or near-globally complete in the modern period.

To include shorter datasets, which can help to better understand recent temperature changes, in the present report, the estimate made by the IPCC for the temperature change between 1850–1900 and 1981–2010 is combined with estimated changes between 1981–2010 and the current year from six datasets – HadCRUT5, Berkeley Earth, NOAA GlobalTemp v6, GISTEMP, ERA5 and JRA-3Q (see below) – to calculate anomalies for 2024 relative to 1850–1900. There is good agreement among the datasets on changes from 1981–2010 to the present, as this is a period with good observational coverage. The additional uncertainty from the spread of the datasets is combined with that of the IPCC's estimate of the uncertainty in the change from 1850–1900 to 1981–2010.

Global mean temperature anomalies were calculated relative to an 1850–1900 baseline using the following steps starting from the time series of global monthly mean temperatures for each dataset:

1. For each dataset, anomalies were calculated relative to the 1981–2010 average by subtracting the mean for the period 1981–2010 for each month separately.
2. An annual mean anomaly was calculated from the monthly mean anomalies.
3. The amount of 0.69 °C was added to each series, based on the estimated difference between 1850–1900 and 1981–2010, calculated using the method from IPCC AR6 WG I (see the caption for Figure 1.12 in that report).
4. The mean and standard deviation of the estimates were calculated.
5. The uncertainty in the IPCC estimate was combined with the standard deviation, assuming the two are independent and assuming the IPCC uncertainty range (0.54 °C–0.79 °C) is representative of a 90% confidence range (1.645 standard deviations).

The number quoted in this report for 2024 (1.55 °C ± 0.13 °C) was calculated in this way, with 1.55 °C being the mean of the six estimates and 0.05 °C the standard deviation.

ANNUAL TEMPERATURE MAPS

For the map of temperature anomalies for 2024, a median of six datasets was used, re-gridded to the spatial grid of the lowest resolution datasets (NOAAGlobalTemp and HadCRUT5), which are presented on a 5° latitude by 5° longitude grid. The median is used in preference to the mean to minimize the effect of potential outliers in individual grid cells. The half-range of the datasets provides an indication of the uncertainty. The spread between the datasets is largest at high latitudes and in Central Africa, both regions with sparse data coverage.

GLOBAL MEAN TEMPERATURE ANOMALIES FOR 2024 RELATIVE TO OTHER PERIODS

Table 1 shows global mean temperature anomalies for individual datasets for 2024 relative to four different baselines. The uncertainties indicated for the three modern baselines (1981–2010, 1991–2020 and 1961–1990) are the standard deviations of the available estimates multiplied by 1.645 to represent the 90% uncertainty range.

Table 1. Global mean temperature anomalies for individual datasets for 2024 for four different baselines

<i>Period</i>	<i>1850–1900</i>	<i>1981–2010</i>	<i>1991–2020</i>	<i>1961–1990</i>
HadCRUT5	1.52	0.83	0.63	1.17
NOAA GlobalTemp	1.53	0.84	0.66	1.15
GISTEMP	1.55	0.86	0.67	1.18
Berkeley Earth	1.54	0.85	0.65	1.20
ERA5	1.60	0.91	0.72	1.24
JRA-3Q	1.57	0.88	0.69	1.21
Mean of the six datasets	1.55 ± 0.13	0.86 ± 0.05	0.67 ± 0.05	1.19 ± 0.05

The following six datasets were used, including four traditional datasets:

- Berkeley Earth: Rohde, R. A.; Hausfather, Z. The Berkeley Earth Land/Ocean Temperature Record. *Earth System Science Data* **2020**, 12 (4), 3469–3479. <https://doi.org/10.5194/essd-12-3469-2020>.
- GISTEMP v4: GISTEMP Team, 2022: *GISS Surface Temperature Analysis (GISTEMP), version 4*. NASA Goddard Institute for Space Studies, <https://data.giss.nasa.gov/gistemp/>. Lenssen, N.; Schmidt, G.; Hansen, J. et al. Improvements in the GISTEMP Uncertainty Model. *Journal of Geophysical Research: Atmospheres* **2019**, 124 (12), 6307–6326. <https://doi.org/10.1029/2018JD029522>.
- HadCRUT.5.0.2.0: Morice, C. P.; Kennedy, J. J.; Rayner, N. A. et al. An Updated Assessment of Near-Surface Temperature Change From 1850: The HadCRUT5 Data Set. *Journal of Geophysical Research: Atmospheres* **2021**, 126 (3), e2019JD032361. <https://doi.org/10.1029/2019JD032361>. HadCRUT.5.0.2.0 data were obtained from <http://www.metoffice.gov.uk/hadobs/hadcrut5> on 19 January 2025 and are © British Crown Copyright, Met Office 2025, provided under an Open Government Licence, <http://www.nationalarchives.gov.uk/doc/open-government-licence/version/3/>.
- NOAA v6: Huang, B.; Yin, X.; Menne, M. J. et al. *NOAA Global Surface Temperature Dataset (NOAGlobalTemp)*, Version 6.0.0. NOAA National Centers for Environmental Information, 2025. <https://doi.org/10.25921/rzxcg-p717>.

And two reanalyses:

- ERA5: Hersbach, H.; Bell, B.; Berrisford, P. et al. *ERA5 Monthly Averaged Data on Single Levels from 1940 to Present*; Copernicus Climate Change Service (C3S) Climate Data Store (CDS), 2023. <https://doi.org/10.24381/cds.f17050d7>.
- JRA-3Q: Kosaka, Y.; Kobayashi, S.; Harada, Y. et al. The JRA-3Q Reanalysis. *Journal of the Meteorological Society of Japan, Ser. II* **2024**, 102 (1), 49–109. <https://doi.org/10.2151/jmsj.2024-004>.

IPCC used an additional dataset:

- Kadow et al.: Kadow, C.; Hall, D. M.; Ulbrich, U. Artificial Intelligence Reconstructs Missing Climate Information. *Nature Geoscience* **2020** 13, 408–413. <https://doi.org/10.1038/s41561-020-0582-5>.

OCEAN HEAT CONTENT DATA

Note that global ocean heat content values are given for the ocean surface area between 60 °S–60 °N and limited to areas deeper than 300 m. A baseline of 2005–2021 is used for the ocean heat content time series as near-global coverage is available for this period thanks to the network of Argo subsurface floats. Warming rates in watts per square metre refer to the ocean surface area. To get a number for the entire surface of the globe (as used, for example, in the United Nations Educational, Scientific and Cultural Organization (UNESCO) State of the Ocean report) multiply by 0.71. Ocean heat content changes are given in two sets of units: watts per square metre and zettajoules (ZJ) per year (1 W m⁻² corresponds to 11.35 ZJ per year).

The assessment for 2024 is based on the following three datasets:

- Cheng, L.; Pan, Y.; Tan, Z. et al. IAPv4 Ocean Temperature and Ocean Heat Content Gridded Dataset. *Earth System Science Data* **2024**, 16 (8), 3517–3546. <https://doi.org/10.5194/essd-16-3517-2024>.

Minière, A.; von Schuckmann, K.; Sallée, J.-B. et al. Robust Acceleration of Earth System Heating Observed over the Past Six Decades. *Scientific Reports* **2023**, *13*, 22975. <https://doi.org/10.1038/s41598-023-49353-1>.

von Schuckmann, K.; Le Traon, P.-Y. How Well Can We Derive Global Ocean Indicators from Argo Data? *Ocean Science* **2011**, *7* (6), 783–791. <https://doi.org/10.5194/os-7-783-2011>.

SEA-LEVEL DATA

GMSL from CNES/Aviso+, <https://www.aviso.altimetry.fr/en/data/products/ocean-indicators-products/mean-sea-level/data-acces.html#c12195>.

OCEAN pH DATA

This indicator is produced by the Copernicus Marine Service. References include:

Chau, T. T. T.; Gehlen, M.; Chevallier, F. A Seamless Ensemble-based Reconstruction of Surface Ocean pCO₂ and Air–Sea CO₂ Fluxes over the Global Coastal and Open Oceans. *Biogeosciences* **2022**, *19*, 1087–1109. <https://doi.org/10.5194/bg-19-1087-2022>.

Gehlen M.; Chau, T. T. T.; Conchon, A. et al. Ocean Acidification. *Journal of Operational Oceanography* **2020**, *13* (sup1), s88–s91. <https://doi.org/10.1080/1755876X.2020.1785097>.

GLACIER DATA

Global glacier monitoring information is provided by the World Glacier Monitoring Service:

World Glacier Monitoring Service (WGMS), 2024: *Fluctuations of Glaciers Database*. WGMS, Zurich, Switzerland. <https://doi.org/10.5904/wgms-fog-2024-01>.

SEA-ICE DATA

Data are from the European Organization for the Exploitation of Meteorological Satellites (EUMETSAT) Ocean and Sea Ice Satellite Application Facility (OSI SAF) Sea-Ice Index v2.2 (based on Lavergne et al., 2019; <https://osisaf-hl.met.no/v2p2-sea-ice-index>) and the National Snow and Ice Data Center (NSIDC) v3 Sea Ice Index (Fetterer et al., 2017). Sea-ice concentrations are estimated from microwave radiances measured from satellites. Extent is the area of ocean grid cells where the sea-ice concentration exceeds 15%. There are modest differences in the absolute extent between datasets, but they agree well on the year-to-year changes and trends. In the main text of the present report, NSIDC values are reported for absolute extents, and rankings. Comparison figures for OSI SAF are given in Table 2.

Table 2. NSIDC values compared with EUMETSAT Ocean and Sea Ice Satellite Application Facility figures for 2024

<i>Metric</i>	<i>NSIDC</i>	<i>OSI SAF</i>
Arctic daily minimum	4.28 million km ² , 11 September	4.64 million km ² , 13 September
Arctic daily maximum	15.01 million km ² , 14 March	15.02 million km ² , 11 March
Antarctic daily minimum	1.99 million km ² , 20 February	2.24 million km ² , 18 February
Antarctic daily maximum	17.16 million km ² , 19 September	17.65 million km ² , 28 September

European Organization for the Exploitation of Meteorological Satellites (EUMETSAT) Ocean and Sea Ice Satellite Application Facility (OSI SAF). *Sea Ice Index 1978–Onwards, Version 2.2, OSI-420*. EUMETSAT OSI SAF, 2023. Data extracted from OSI SAF FTP server: (1978–2025).

Fetterer, F.; Knowles, K.; Meier, W. N. et al. *Sea Ice Index, Version 3*. National Snow and Ice Data Center (NSIDC): Boulder, USA, 2017. <https://nsidc.org/data/G02135/versions/3>.

Lavergne, T.; Sørensen, A. M.; Kern, S. et al. Version 2 of the EUMETSAT OSI SAF and ESA CCI Sea-ice Concentration Climate Data Records. *The Cryosphere* **2019**, 13 (1), 49–78. <https://doi.org/10.5194/tc-13-49-2019>.

PRECIPITATION DATA

The following Global Precipitation Climatology Centre (GPCC) datasets were used in the analysis:

- First Guess Monthly, https://doi.org/10.5676/DWD_GPCC/FG_M_100
- Monitoring Product (Version 2022), https://doi.org/10.5676/DWD_GPCC/MP_M_V2022_100
- Full Data Monthly (Version 2022), https://doi.org/10.5676/DWD_GPCC/FD_M_V2022_100
- Precipitation Climatology (Version 2022), https://doi.org/10.5676/DWD_GPCC/CLIM_M_V2022_100

ENSO MAP

The map of typical El Niño impacts on precipitation was based on information from various sources, including:

- <https://iridl.ldeo.columbia.edu/maproom/IFRC/FIC/ElNinoandRainfall.pdf>
- https://interagencystandingcommittee.org/sites/default/files/migrated/2019-02/inter_agency_sops_for_early_action_to_el_nino_la_nina_episodes.pdf
- <https://www.metoffice.gov.uk/binaries/content/gallery/metofficegovuk/images/research/climate/global/el-nino-precip.jpg>
- <https://climexp.knmi.nl/effects.cgi?id=someone@somewhere#precipitation>
- https://ds.data.jma.go.jp/tcc/tcc/products/climate/ENSO/el_nino.html
- <https://confluence.ecmwf.int/display/COPSRV/ENSO+impacts+on+Europe>
- Famine Early Warning Systems Network (FEWS NET). *El Niño and Precipitation; Agroclimatology Fact Sheet Series; Vol. 1; 2020*.

SIDE BAR –

GLOBAL MEAN SURFACE TEMPERATURE ANOMALIES IN 2023/2024: TOWARDS UNDERSTANDING THE INFLUENCING FACTORS

The global temperature series used is the average of the six global temperature datasets described in [Global temperature data](#). The smoothly rising trend was estimated using a 20-year loess smoothed curve fitted to the data through 2022 and projected to 2024.

The impact of ENSO on the temperatures can be estimated in multiple ways. A linear regression of the annual mean relative anomaly on the February/March [Niño 3.4 index](#) is used here and suggests an impact of -0.07°C , 0.01°C and 0.13°C for 2022, 2023 and 2024, respectively (95% CI, $\pm 0.13^{\circ}\text{C}$). Some results from pre-industrial control climate model simulations⁵⁶ suggest a transition from triple-dip La Niña to El Niño can produce an anomalous jump of up to 0.25°C in the year of transition, but it is unclear how to apply this to 2023, since one would need to condition the effect on the ENSO change that was actually experienced.

The IMO regulation change in 2020 led to a quick reduction of about 7 TgSO₂ per year and a step change of radiative forcing of $0.15 [0.1-0.2] \text{ W m}^{-2}$ (with a range estimated from a selection of studies^{57,58,59,60,61}). The temperature impacts in 2023 calculated by the respective studies reviewed are between 0.03°C and 0.08°C , and they are slightly larger in 2024.

Solar cycle 25 was both slightly earlier and slightly stronger than [had been expected](#), and the impact of the total solar irradiance (TSI) anomaly of 0.97 W m^{-2} in 2023 relative to the mean of the prior 20 years is a radiative forcing of approximately 0.17 W m^{-2} and an estimated impact of $0.07^{\circ}\text{C} [0.05-0.10]^{\circ}\text{C}$ on surface global mean temperatures with a one to two year lag.⁶² Thus, the impacts on 2023 and 2024 are around 0.04°C and 0.07°C , respectively ($\pm 0.025^{\circ}\text{C}$).

[East Asian sulfate aerosol emissions](#) have fallen sharply from their peak in 2006 (38 TgSO₂ per year) – a third by 2014 (23 TgSO₂ per year) and then by an additional 50% since then (in 2022 it was 11 TgSO₂ per year). On its own this would lead to additional radiative forcing of 0.14 W m^{-2} and warming of $0.06^{\circ}\text{C} (\pm 0.04^{\circ}\text{C})$ in 2023 compared to a world where East Asian aerosol emissions remained at 2006 levels. But some of this decline will have already affected the long-term trends, and so the anomaly in 2023 relative to 2020 is only 0.01°C (calculated using the Finite Amplitude Impulse Response (FaIR) model⁶³ (Leach et al., 2021)).

The HTHH volcanic event added both SO₂ and water vapour to the stratosphere (up to 56 km in altitude). The rapid oxidation of SO₂ to sulfate aerosol dominated the radiative forcing for the first two years after the eruption, and so the net radiative forcing at the tropopause was likely negative: -0.04 W m^{-2} and -0.15 W m^{-2} in 2022 and 2023, respectively,⁶⁴ implying a temperature impact of $-0.02^{\circ}\text{C} [-0.01^{\circ}\text{C} \text{ to } -0.03^{\circ}\text{C}]$, calculated using the FaIR model.

List of contributors

CONTRIBUTING MEMBERS

Algeria, Argentina, Armenia, Australia, Azerbaijan, Bahrain, Bangladesh, Barbados, Belgium, Belize, Benin, Bosnia and Herzegovina, Botswana, Brazil, Brunei Darussalam, Bulgaria, Cameroon, Canada, Chile, China, Comoros, Costa Rica, Côte d'Ivoire, Croatia, Cuba, Cyprus, Czechia, Denmark, Democratic Republic of the Congo, Dominica, Dominican Republic, Ecuador, Egypt, El Salvador, Estonia, Eswatini, Finland, France, Germany, Ghana, Greece, Guatemala, Guinea-Bissau, Hong Kong, China; Iceland, India, Islamic Republic of Iran, Iraq, Ireland, Israel, Italy, Japan, Kazakhstan, Kenya, Latvia, Libya, Lithuania, Macao, China; Malawi, Malaysia, Mali, Mauritius, Monaco, Morocco, Mozambique, Myanmar, Namibia, Kingdom of the Netherlands, New Zealand, Norway, Pakistan, Paraguay, Peru, Philippines, Poland, Portugal, Republic of Korea, Republic of Moldova, Russian Federation, Rwanda, Saint Vincent and the Grenadines, Saudi Arabia, Senegal, Serbia, Singapore, Slovakia, Slovenia, South Africa, Sudan, Sweden, Switzerland, Syrian Arab Republic, Thailand, Trinidad and Tobago, Tunisia, Türkiye, Ukraine, United Kingdom of Great Britain and Northern Ireland, United Republic of Tanzania, United States of America, Uruguay

UN AGENCIES

Food and Agriculture Organization of the United Nations (FAO), International Organization for Migration (IOM), United Nations High Commissioner for Refugees (UNHCR)

INSTITUTIONS AND DATA PROVIDERS

Archiving, Validation and Interpretation of Satellite Oceanographic data (AVISO), France; Berkeley Earth, USA; Bureau of Meteorology (BOM), Australia; CELAD, France; Climatic Research Unit (CRU), University of East Anglia, UK; Commonwealth Scientific and Industrial Research Organisation (CSIRO), Australia; Cooperative Institute for Research in Environmental Sciences (CIRES), University of Colorado, Boulder, USA; Copernicus Marine Environment Monitoring Service (CMEMS); Ecole Nationale Supérieure (ENS), France; Egyptian Meteorological Authority; Environment and Climate Change Canada (ECCC); European Centre for Medium-Range Weather Forecasts (ECMWF); European Organization for the Exploitation of Meteorological Satellites (EUMETSAT) Ocean and Sea Ice Satellite Application Facility (OSI SAF); Global Precipitation Climatology Centre (GPCC), Germany; Graduate School of International Studies (GSIS), Korea University; Institute of Atmospheric Physics (IAP), Chinese Academy of Sciences (CAS); Instituto Português do Mar e da Atmosfera (IPMA); Integrated Carbon Observation System (ICOS) – European Research Infrastructure Consortium (ERIC)/Lund University, Sweden; Internal Displacement Monitoring Centre (IDMC); Japan Meteorological Agency (JMA); Laboratoire de Météorologie Dynamique (LMD), France; Laboratoire des Sciences du Climat et de l'Environnement (LSCE), France; Max Planck Institute (MPI) for Biogeochemistry, Germany; Mercator Ocean International, France; Met Office Hadley Centre, UK; National Aeronautics and Space Administration (NASA) Goddard Institute for Space Studies (GISS), USA; NOAA Global Monitoring Laboratory (GML), USA; NOAA National Centers for Environmental Information (NCEI), USA; National Snow and Ice Data Center (NSIDC), USA; Scripps Institution of Oceanography, University of California, San Diego, USA; Stripe, Inc., USA; Turkish State Meteorological Service (TSMS); Universidade Estadual Paulista/Centro Nacional de Monitoramento e Alertas de Desastres Naturais (UNESP/CEMADEN), Brazil; Universidade Federal do Rio de Janeiro (UFRJ), Brazil; University of Bremen, Germany; University of California, Los Angeles (UCLA), USA; Wageningen University and Research, Kingdom of the Netherlands; World Data Centre for Greenhouse Gases (WDCGG); World Glacier Monitoring Service (WGMS)

SECTION AUTHORS

Lead author and scientific coordinator – John Kennedy (WMO)

Carbon dioxide – Oksana Tarasova (WMO), Alex Vermeulen (ICOS ERIC), Xin Lan (NOAA GML, CIRES), Kazuhiro Tsuboi (JMA, WDCGG), Andrew Crotwell (NOAA GML, CIRES), Christoph Gerbig (MPI), Armin Jordan (MPI), Zoë Loh (CSIRO), Ingrid Luijkx (Wageningen University and Research), John Miller (NOAA GML), Ray Weiss (Scripps Institution of Oceanography), Thorsten Warneke (University of Bremen, Germany), Camille Yver (LSCE)

Global mean temperature – John Kennedy (WMO)

Ocean heat content – Karina von Schuckmann (Mercator Ocean international), Audrey Minière (ENS, LMD), Lijing Cheng (IAP/CAS), Flora Gues (CELAD)

Global mean sea level – Anny Cazenave (Laboratoire d'Etudes en Géophysique et Océanographie Spatiales (LEGOS)), Lancelot Leclercq (LEGOS)

Ocean pH – Karina von Schuckmann (Mercator Ocean international), Flora Gues (CELAD)

Glacier mass balance – Shawn Marshall (ECCC)

Sea-ice extent – Shawn Marshall (ECCC)

El Niño–Southern Oscillation – Jessica Blunden (NOAA NCEI)

Global patterns of temperature and precipitation – Markus Ziese (GPCC, DWD), John Kennedy (WMO)

High-impact events – Blair Trewin (BOM), Jorge Alvar-Beltran (FAO), Arianna Gialletti (FAO), Jana Birner (UNHCR), Rosi-Selam Reusing (UNHCR), Elisabeth du Parc (IOM), Vicente Anzellini (IDMC), Sylvain Ponserre (IDMC)

Monitoring global temperature for the Paris Agreement – Richard Betts (University of Exeter and Met Office Hadley Centre), Fatima Driouech (University Mohammed VI Polytechnic (UM6P)), Robert Dunn (Met Office Hadley Centre), Piers Forster (University of Leeds), Yu-Kyung Hyun (Korea Meteorological Administration), Jose Marengo (UNESP/CEMADEN, GSIS), Karen McKinnon (UCLA), Colin Morice (Met Office Hadley Centre), Matthew Palmer (Met Office Hadley Centre and University of Bristol), Chris Smith (Vrije Universiteit Brussel), Peter Thorne (Irish Climate Analysis and Research UnitS (ICARUS) Climate Research Centre, Maynooth University), Blair Trewin (BOM), Tristram Walsh (University of Oxford), Jonathan Winn (Met Office Hadley Centre), Panmao Zhai (Chinese Academy of Meteorological Sciences)

Sidebar: Global mean temperature anomalies in 2023/2024 – Gavin A. Schmidt (NASA GISS), Zeke Hausfather, (Stripe, Inc.)

REVIEWERS

Omar Baddour (WMO), Jesse Cruz (WMO), Nilay Dogulu (WMO), Robert Dunn (Met Office Hadley Centre), Awatif Ebrahim (Egyptian Meteorological Authority), Veronica Grasso (WMO), Peer Hechler (WMO), Christopher Hewitt (WMO), Anahit Hovsepyan (WMO), Andries Kruger (South African Weather Service), Renata Libonati (UFRJ), Belén Martin Míguez (WMO), Atsushi Minami (JMA), Nakiete Msemo (WMO), Clare Nullis (WMO), Claire Ransom (WMO), Serhat Sensoy (TSMS), Peter Siegmund (KNMI), Álvaro Silva (IPMA), Mxolisi Shongwe (Intergovernmental Panel on Climate Change (IPCC)), Michael Sparrow (WMO), Johan Stander (WMO), Peter Thorne (Maynooth University), Blair Trewin (BOM), Freja Vamborg (ECMWF), Robert Vautard (IPCC)

WMO PROGRAMME COORDINATION

Omar Baddour (Chief, Climate Monitoring and Policy Services (CMP)), Claire Ransom (Associate Scientific Officer, CMP), Peer Hechler (Scientific Officer, CMP), Amir Delju (Senior Scientific Officer, Services), Wilfran Moufouma Okia (Chief, Regional Climate Prediction Services (RCP)), Saeed Vazifehkhah (Scientific Officer, RCP), Benjamin Welch (CMP)

Endnotes

- ¹ World Meteorological Organization (WMO). *WMO Greenhouse Gas Bulletin, No. 20: The State of Greenhouse Gases in the Atmosphere Based on Global Observations through 2023*; WMO: Geneva, 2024.
- ² Montzka, S. A. *The NOAA Annual Greenhouse Gas Index (AGGI)*; National Oceanic and Atmospheric Administration (NOAA) Earth System Research Laboratories Global Monitoring Laboratory, 2024. <http://www.esrl.noaa.gov/gmd/aggi/aggi.html>.
- ³ Intergovernmental Panel on Climate Change (IPCC). *Climate Change 2021: The Physical Science Basis. Contribution of Working Group I to the Sixth Assessment Report of the Intergovernmental Panel on Climate Change*; Masson-Delmotte, V.; Zhai, P.; Pirani, A. et al., Eds.; Cambridge University Press: Cambridge, UK and New York, USA, 2021. <https://doi.org/10.1017/9781009157896>.
- ⁴ Friedlingstein, P.; O’Sullivan, M.; Jones, M. W. et al. Global Carbon Budget 2024. *Earth System Science Data* **2024** [preprint]. <https://doi.org/10.5194/essd-2024-519>.
- ⁵ Intergovernmental Panel on Climate Change (IPCC). *Climate Change 2021: The Physical Science Basis. Contribution of Working Group I to the Sixth Assessment Report of the Intergovernmental Panel on Climate Change*; Masson-Delmotte, V.; Zhai, P.; Pirani, A. et al., Eds.; Cambridge University Press: Cambridge, UK and New York, USA, 2021. <https://doi.org/10.1017/9781009157896>.
- ⁶ von Schuckmann, K.; Minière, A.; Gues, F. et al. Heat Stored in the Earth System 1960–2020: Where Does the Energy Go? *Earth System Science Data* **2023**, 15(4), 1675–1709. <https://doi.org/10.1029/2012GL051106>.
- ⁷ Levitus, S.; Antonov, J. I.; Boyer, T. P. et al. World Ocean Heat Content and Thermosteric Sea Level Change (0–2000 m), 1955–2010. *Geophysical Research Letters* **2012**, 39(10). <https://doi.org/10.1029/2012GL051106>.
- ⁸ Cheng, L.; von Schuckmann, K.; Abraham, J. P. et al. Past and Future Ocean Warming. *Nature Reviews Earth & Environment* **2022**, 3, 776–794. <https://doi.org/10.1038/s43017-022-00345-1>.
- ⁹ Intergovernmental Panel on Climate Change (IPCC). *Climate Change 2021: The Physical Science Basis. Contribution of Working Group I to the Sixth Assessment Report of the Intergovernmental Panel on Climate Change*; Masson-Delmotte, V.; Zhai, P.; Pirani, A. et al., Eds.; Cambridge University Press: Cambridge, UK and New York, USA, 2021. <https://doi.org/10.1017/9781009157896>.
- ¹⁰ Intergovernmental Panel on Climate Change (IPCC). *IPCC Special Report on the Ocean and Cryosphere in a Changing Climate*; Pörtner, H.-O.; Roberts, D. C.; Masson-Delmotte, V. et al., Eds.; Cambridge University Press: Cambridge, UK and New York, USA, 2019. <https://doi.org/10.1017/9781009157964>.
- ¹¹ Piecuch, C. G.; Quinn, K. J. El Niño, La Niña, and the Global Sea Level Budget. *Ocean Science* **2016**, 12, 1165–1177. <https://doi.org/10.5194/os-12-1165-2016>.
- ¹² WCRP Global Sea Level Budget Group. Global Sea-level Budget 1993–present. *Earth System Science Data* **2018**, 10, 1551–1590. <https://doi.org/10.5194/essd-10-1551-2018>.
- ¹³ Intergovernmental Panel on Climate Change (IPCC). *Climate Change 2022: Impacts, Adaptation and Vulnerability. Contribution of Working Group II to the Sixth Assessment Report of the Intergovernmental Panel on Climate Change*; Pörtner, H.-O.; Roberts, D. C.; Tignor, M. et al., Eds.; Cambridge University Press: Cambridge, UK and New York, USA, 2022. <https://doi.org/10.1017/9781009325844>.
- ¹⁴ Intergovernmental Panel on Climate Change (IPCC). *Climate Change 2021: The Physical Science Basis. Contribution of Working Group I to the Sixth Assessment Report of the Intergovernmental Panel on Climate Change*; Masson-Delmotte, V.; Zhai, P.; Pirani, A. et al., Eds.; Cambridge University Press: Cambridge, UK and New York, USA, 2021. <https://doi.org/10.1017/9781009157896>.
- ¹⁵ von Schuckmann, K.; Moreira, L.; Cancet, M. et al. The State of the Global Ocean. In: *Copernicus Ocean State Report*, 8th edition; von Schuckmann, K.; Moreira, L.; Grégoire, M. et al., Eds.; Copernicus Publications, 2024. <https://doi.org/10.5194/sp-4-osr8-1-2024>.
- ¹⁶ Friedlingstein, P.; O’Sullivan, M.; Jones, M. W. et al. Global Carbon Budget 2024. *Earth System Science Data* **2024** [preprint]. <https://doi.org/10.5194/essd-2024-519>.

- ¹⁷ Intergovernmental Panel on Climate Change (IPCC). Summary for Policymakers. In: *Climate Change 2021: The Physical Science Basis. Contribution of Working Group I to the Sixth Assessment Report of the Intergovernmental Panel on Climate Change*; Masson-Delmotte, V.; Zhai, P.; Pirani, A. et al., Eds.; Cambridge University Press: Cambridge, UK and New York, USA, <https://doi.org/10.1017/9781009157896.001>.
- ¹⁸ Bindoff, N. L.; Cheung, W. W. L.; Kairo, J. G. et al. Changing Ocean, Marine Ecosystems, and Dependent Communities. In: *IPCC Special Report on the Ocean and Cryosphere in a Changing Climate*; Pörtner, H.-O.; Roberts, D. C.; Masson-Delmotte, V. et al., Eds.; Cambridge University Press: Cambridge, UK and New York, USA, 2019. <https://doi.org/10.1017/9781009157964.007>.
- ¹⁹ Intergovernmental Panel on Climate Change (IPCC). Summary for Policymakers. In *Climate Change 2022: Impacts, Adaptation, and Vulnerability. Contribution of Working Group II to the Sixth Assessment Report of the Intergovernmental Panel on Climate Change*; Pörtner, H.-O.; Roberts, D. C.; Tignor, M. et al., Eds.; Cambridge University Press: Cambridge, UK and New York, USA, 2022. <https://doi.org/10.1017/9781009325844.001>.
- ²⁰ Intergovernmental Panel on Climate Change (IPCC). Summary for Policymakers. In *IPCC Special Report on the Ocean and Cryosphere in a Changing Climate*; Pörtner, H.-O.; Roberts, D. C.; Masson-Delmotte, V. et al., Eds.; Cambridge University Press: Cambridge, UK and New York, USA, 2019. <https://doi.org/10.1017/9781009157964.001>.
- ²¹ WCRP Global Sea Level Budget Group. Global Sea-level Budget 1993–present. *Earth System Science Data* **2018**, *10*, 1551–1590. <https://doi.org/10.5194/essd-10-1551-2018>.
- ²² Intergovernmental Panel on Climate Change (IPCC). Summary for Policymakers. In: *Climate Change 2021: The Physical Science Basis. Contribution of Working Group I to the Sixth Assessment Report of the Intergovernmental Panel on Climate Change*; Masson-Delmotte, V.; Zhai, P.; Pirani, A. et al., Eds.; Cambridge University Press: Cambridge, UK and New York, USA, 2021. <https://doi.org/10.1017/9781009157896.001>.
- ²³ National Snow and Ice Data Center (NSIDC). *2024 Antarctic Sea Ice Maximum Extent Finishes at Second Lowest*; NSIDC, 3 October 2024. <https://nsidc.org/sea-ice-today/analyses/2024-antarctic-sea-ice-maximum-extent-finishes-second-lowest>.
- ²⁴ Purich, A.; Doddridge, E. W. Record Low Antarctic Sea Ice Coverage Indicates a New Sea Ice State. *Communications Earth & Environment* **2023**, *4* (1). <https://doi.org/10.1038/s43247-023-00961-9>.
- ²⁵ Dinneen, J. Another Extreme Low for Antarctic Sea Ice Signals a Permanent Shift. *New Scientist*, 12 September 2024. <https://www.newscientist.com/article/2447700>.
- ²⁶ <https://www.fsinplatform.org/sites/default/files/resources/files/GRFC2024-MYU-en.pdf>
- ²⁷ EM-DAT lists 890 deaths in 6 countries
- ²⁸ <https://ahacentre.org/situation-update/situation-update-no-8-combined-effects-of-tropical-cyclone-yagi-and-southwest-monsoon-27-september-2024/>
- ²⁹ A total of 219 deaths according to <https://www.ncei.noaa.gov/access/billions/events/US/2024>
- ³⁰ Preliminary Internal Displacement Monitoring Centre (IDMC) figures
- ³¹ <https://www.unhcr.org/news/briefing-notes/cyclone-chido-leaves-trail-destruction-mozambique-and-beyond-displacing>
- ³² <https://reliefweb.int/report/mayotte-france/acaps-briefing-note-mayotte-impact-tropical-cyclone-chido-19-december-2024>
- ³³ <https://reliefweb.int/report/mayotte-france/situation-overview-overview-impact-cyclone-chido-mayotte-18122024>
- ³⁴ Food and Agriculture Organization of the United Nations (FAO). *Floods in Afghanistan, 2024: The Impact of the Floods on Agriculture and Livelihoods*; FAO Data in Emergencies Hub, 2024.
- ³⁵ <https://www.unhcr.org/news/briefing-notes/flood-hit-communities-afghanistan-need-urgent-humanitarian-support>
- ³⁶ Food and Agriculture Organization of the United Nations (FAO). *Flooding in the Sahel Countries: What Impact on Agriculture and Food Security?* FAO, 2024. <https://www.fao.org/africa/news-stories/news-detail/flooding-in-the-sahel-countries--what-impact-on-agriculture-and-food-security/en>.

- ³⁷ <https://www.unocha.org/publications/report/kenya/eastern-africa-heavy-rains-and-flooding-flash-update-1-3-may-2024>
- ³⁸ <https://www.unhcr.org/news/stories/five-things-know-about-catastrophic-flooding-east-and-horn-africa>
- ³⁹ <https://reliefweb.int/report/kenya/eastern-africa-heavy-rains-and-flooding-flash-update-4-30-may-2024>
- ⁴⁰ <https://www.unhcr.org/sites/default/files/2024-09/Southern-Africa-75-ExCom-English.pdf>
- ⁴¹ <https://reliefweb.int/report/zambia/unhcr-zambia-drought-emergency-update-no-1-31-july-2024>
- ⁴² EM-DAT
- ⁴³ <https://www.canada.ca/en/environment-climate-change/services/ten-most-impactful-weather-stories/2024.html>
- ⁴⁴ <https://atmosphere.copernicus.eu/cams-global-wildfires-review-2024-harsh-year-americas>
- ⁴⁵ Preliminary Internal Displacement Monitoring Centre (IDMC) data, Global Report on Internal Displacement (GRID) 2025
- ⁴⁶ Thiem, H. *Multi-year Drought and Heat Waves Across Mexico in 2024*; National Oceanic and Atmospheric Administration (NOAA), 22 July 2024. <https://www.climate.gov/news-features/event-tracker/multi-year-drought-and-heat-waves-across-mexico-2024#:~:text=2024's%20drought%20impacts%20on%20crops,directly%20due%20to%20the%20drought.>
- ⁴⁷ <https://www.unhcr.org/news/briefing-notes/unhcr-supports-brazils-response-devastating-floods>
- ⁴⁸ EM-DAT
- ⁴⁹ <https://www.lamoncloa.gob.es/info-dana/Paginas/2024/131224-datos-seguimiento-actuaciones-gobierno.aspx>
- ⁵⁰ World Meteorological Organization (WMO). *2023 State of Climate Services: Health* (WMO-No. 1335). Geneva, 2023.
- ⁵¹ Betts, R. A.; Belcher, S. E.; Hermanson, L. et al. Approaching 1.5 °C: How Will We Know We've Reached This Crucial Warming Mark? *Nature* **2023**, 624 (7990), 33–35. <https://doi.org/10.1038/d41586-023-03775-z>.
- ⁵² Betts, R. A.; Belcher, S. E.; Hermanson, L. et al. Approaching 1.5 °C: How Will We Know We've Reached This Crucial Warming Mark? *Nature* **2023**, 624 (7990), 33–35. <https://doi.org/10.1038/d41586-023-03775-z>.
- ⁵³ Forster, P. M.; Smith, C.; Walsh, T. et al. Indicators of Global Climate Change 2023: Annual Update of Key Indicators of the State of the Climate System and Human Influence. *Earth System Science Data* **2024**, 16 (6), 2625–2658. <https://doi.org/10.5194/essd-16-2625-2024>.
- ⁵⁴ Rantanen, M.; Laaksonen, A. The Jump in Global Temperatures in September 2023 is Extremely Unlikely Due to Internal Climate Variability Alone. *npj Climate and Atmospheric Science* **2024**, 7. <https://doi.org/10.1038/s41612-024-00582-9>.
- ⁵⁵ Intergovernmental Panel on Climate Change (IPCC). *Climate Change 2021: The Physical Science Basis. Contribution of Working Group I to the Sixth Assessment Report of the Intergovernmental Panel on Climate Change*; Masson-Delmotte, V.; Zhai, P.; Pirani, A. et al., Eds.; Cambridge University Press: Cambridge, UK and New York, USA, 2021. <https://doi.org/10.1017/9781009157896>.
- ⁵⁶ Raghuraman, S. P.; Soden, B.; Clement, A. et al. The 2023 Global Warming Spike was Driven by the El Niño–Southern Oscillation. *Atmospheric Chemistry and Physics* **2024**, 24, 11275–11283. <http://dx.doi.org/10.5194/acp-24-11275-2024>.
- ⁵⁷ Gettelman, A.; Christensen, M. W.; Diamond, M. S. et al. Has Reducing Ship Emissions Brought Forward Global Warming? *Geophysical Research Letters* **2024**, 51. <https://doi.org/10.1029/2024GL109077>.
- ⁵⁸ Jordan, G.; Henry, M. IMO2020 Regulations Accelerate Global Warming by up to 3 Years in UKESM1. *Earth's Future* **2024**, 12. <https://doi.org/10.1029/2024EF005011>.
- ⁵⁹ Quaglia, I.; Visioni, D. Modeling 2020 Regulatory Changes in International Shipping Emissions Helps Explain 2023 Anomalous Warming. *The EGU Interactive Community Platform* **2024** [preprint]. <https://doi.org/10.5194/egusphere-2024-1417>.
- ⁶⁰ Yoshioka, M.; Grosvenor, D. P.; Booth, B. B. et al. Warming Effects of Reduced Sulfur Emissions from Shipping. *The EGU Interactive Community Platform* **2024** [preprint]. <https://doi.org/10.5194/egusphere-2024-1428>.

- ⁶¹ Yuan, T.; Song, H.; Oreopoulos, L. et al. Abrupt Reduction in Shipping Emission as an Inadvertent Geoengineering Termination Shock Produces Substantial Radiative Warming. *Communications Earth & Environment* **2024**, *5*. <https://doi.org/10.1038/s43247-024-01442-3>.
- ⁶² Misios, S.; Mitchell, D. M.; Gray, L. J. et al. Solar Signals in CMIP-5 Simulations: Effects of Atmosphere–ocean Coupling. *Quarterly Journal of the Royal Meteorological Society* **2016**, *142* (695), 928–941. <https://doi.org/10.1002/qj.2695>.
- ⁶³ Leach, N. J.; Jenkins, S.; Nicholls, Z. et al. FaIRv2.0.0: A Generalized Impulse Response Model for Climate Uncertainty and Future Scenario Exploration. *Geoscientific Model Development* **2021**, *14*, 3007–3036. <https://doi.org/10.5194/gmd-14-3007-2021>.
- ⁶⁴ Schoeberl, M. R.; Wang, Y.; Taha, G. et al. Evolution of the Climate Forcing During the Two Years After the Hunga Tonga-Hunga Ha'apai Eruption. *Journal of Geophysical Research: Atmospheres* **2024**, *129*. <https://doi.org/10.1029/2024JD041296>.



Food and Agriculture Organization
of the United Nations



UNHCR
The UN Refugee Agency



World Food
Programme

For more information, please contact:

World Meteorological Organization

7 bis, avenue de la Paix – P.O. Box 2300 – CH 1211 Geneva 2 – Switzerland

**Strategic Communications Office
Cabinet Office of the Secretary-General**

Tel: +41 (0) 22 730 83 14 – Fax: +41 (0) 22 730 80 27

Email: cpa@wmo.int

wmo.int